Non-Overlapping Schwarz Waveform-Relaxation for Nonlinear Advection-Diffusion Equations

Gander, Martin Jakob; Lunowa, Stephan B.; Rohde, Christian

How to cite

GANDER, Martin Jakob, LUNOWA, Stephan B., ROHDE, Christian. Non-Overlapping Schwarz Waveform-Relaxation for Nonlinear Advection-Diffusion Equations. In: SIAM journal on scientific computing, 2023, vol. 45, n° 1, p. A49–A73. doi: 10.1137/21M1415005

This publication URL: https://archive-ouverte.unige.ch//unige:169047
Publication DOI: 10.1137/21M1415005

SIAM J. SCI. COMPUT.
Vol. 45, No. 1, pp. A49-A73

NON-OVERLAPPING SCHWARZ WAVEFORM-RELAXATION FOR NONLINEAR ADVECTION-DIFFUSION EQUATIONS*

MARTIN J. GANDER†, STEPHAN B. LUNOWA‡, AND CHRISTIAN ROHDE§

Abstract. Nonlinear advection-diffusion equations often arise in the modeling of transport processes. We propose for these equations a non-overlapping domain decomposition algorithm of Schwarz waveform-relaxation (SWR) type. It relies on nonlinear zeroth-order (or Robin) transmission conditions between the sub-domains that ensure the continuity of the converged solution and of its normal flux across the interface. We prove existence of unique iterative solutions and the convergence of the algorithm. We then present a numerical discretization for solving the SWR problems using a forward Euler discretization in time and a finite volume method in space, including a local Newton iteration for solving the nonlinear transmission conditions. Our discrete algorithm is asymptotic preserving, i.e., robust in the vanishing viscosity limit. Finally, we present numerical results that confirm the theoretical findings, in particular the convergence of the algorithm. Moreover, we show that the SWR algorithm can be successfully applied to two-phase flow problems in porous media as paradigms for evolution equations with strongly nonlinear advective and diffusive fluxes.

Key words. domain decomposition, Schwarz waveform-relaxation, nonlinear advection-diffusion equations

MSC codes. 65M55, 35K55, 35L65, 76S05

DOI. 10.1137/21M1415005

1. Introduction.

Nonlinear advection-diffusion equations often arise in the modeling of transport processes, especially in porous media. Typical examples are (enhanced) oil recovery, CO_2 storage, and geothermal energy production. Since measurements of such processes are usually impossible or at best very difficult and thus very rare, numerical simulations are essential for an adequate understanding. The precise formulation of the underlying nonlinear advection-diffusion equations can involve strong heterogeneities due to largely varying physical properties and parameters. In turn, this raises significant mathematical and computational problems, such that the development and analysis of robust discretization methods becomes a non-trivial challenge.

To still reach reasonable performance, a typical approach is the parallelization by a domain decomposition method, which is an established technique for steady problems; see [11, 45, 50, 52] and references therein. Regardless of the chosen discretization method and of the linearization scheme, these methods aim at reducing the

* Submitted to the journal's Methods and Algorithms for Scientific Computing section April 26, 2021; accepted for publication (in revised form) September 6, 2022; published electronically January 25, 2023.

https://doi.org/10.1137/21M1415005

Funding: The work of the second author was supported by Hasselt University (project BOF17NI01), and by the Research Foundation Flanders (FWO, project G051418N). The work of the third author was supported by the German Research Foundation (DFG) under Germany's Excellence Strategy (EXC 2075 - 390740016) and under Project 327154368 - SFB 1313. The work of the first author was supported by the Swiss National Science Foundation (project 20020˙192064).

† Section de Mathématiques, Université de Genève, CH-1211 Genève, Switzerland (Martin.Gander@unige.ch).

‡ Corresponding author. UHasselt – Hasselt University, Computational Mathematics, 3590 Diepenbeek, Belgium (stephan.lunowa@uhasselt.be, stephan.lunowa@tum.de).

§ Institute for Applied Analysis and Numerical Simulation, University of Stuttgart, 70569 Stuttgart, Germany (christian.rohde@mathematik.uni-stuttgart.de).

computational complexity by splitting the domain appropriately into sub-domains and then solving the problem on the single sub-domains iteratively. The convergence is obtained by imposing appropriate transmission conditions between the sub-domains for consecutive iterations. Here we focus on Schwarz waveform-relaxation (SWR) methods, which are time-parallel time integration methods [18] based on waveform-relaxation techniques invented in [39] for VLSI design, and use domain decomposition in space following the seminal work of Schwarz [46] for the parallelization. SWR methods have been studied over the past two decades for many evolution problems, starting with [7, 14, 27, 29] for linear parabolic problems with typical superlinear convergence, and [20, 23] for hyperbolic problems, where these algorithms typically converge in a finite number of steps, and also optimal and optimized transmission conditions were introduced, based on [22]. Such transmission conditions are crucial for good performance, which has been demonstrated, e.g., in [19, 43] for the two-dimensional linear advection-reaction-diffusion equation. Asymptotic expressions for the optimal parameters in the transmission conditions have been analyzed in [5, 6, 21] for linear equations by the Fourier transform; see also [41, 44] for steady advection-diffusion problems with a non-overlapping domain decomposition with Robin transmission conditions. Less is known for the case of nonlinear problems: superlinear convergence was proved in [15] for classical overlapping SWR for semilinear reaction diffusion, and for advection-dominated nonlinear conservation laws in [26]. An analysis of non-overlapping SWR for semilinear wave propagation can be found in [35]. Optimized transmission conditions were explored for nonlinear reactive transport in [33, 34], the latter also containing Newton acceleration. This approach was numerically explored for the Navier–Stokes equations in [10]; see also [30, 31] with transmission conditions from [8] for the error analysis of a (discrete) domain-decomposition algorithm. To the best of our knowledge there are so far no rigorous convergence results for non-overlapping SWR algorithms applied to fully nonlinear advection-diffusion equations.

The purpose of the present paper is to provide a theory for non-overlapping SWR algorithms with Robin transmission conditions applied to nonlinear advection-diffusion problems in time and space; see problem (2.1)–(2.3). For the resulting algorithm on two sub-domains we rigorously prove convergence. Our approach exploits the weak solution concept as it has been established for quasi-linear elliptic-parabolic equations in the seminal work by Alt and Luckhaus [3]. In this way we work in the most general framework induced by the generic energy estimates on nonlinear advection-diffusion equations. Our convergence analysis follows the lines of Caetano et al. in [9], where non-overlapping SWR algorithms were considered for nonlinear reaction-diffusion equations. However, the chosen concept of weak solutions allows us to avoid higher-order regularity results and the use of fixed point arguments.

Our paper is structured as follows: we first present the problem on the entire domain, the non-overlapping SWR algorithm, and weak solution concepts in section 2. In section 3, we deal with the existence and (imposing stronger assumptions on data) uniqueness of weak solutions for the SWR problems. On this basis, we proceed in section 4 with the proof of the convergence of these solutions towards the solution of the problem on the entire domain. This main result is formulated in Theorem 4.1. In section 5, we present the numerical treatment of the equations and a fully discrete SWR algorithm that relies on a finite volume approach on triangular meshes in two spatial dimensions. In particular, our design of the discrete Robin transmission conditions is asymptotic preserving; i.e., in the hyperbolic limit, we recover the desired fast hyperbolic convergence of the method in a finite number of iterations. Finally, in section 6 we illustrate the theoretical convergence results by

numerical examples and provide numerical simulations for two-phase flow in porous media, including problems with strong nonlinearities.

2. Problem description and the non-overlapping Schwarz waveform-relaxation algorithm. For $d \in \mathbb{N}$ let $\Omega \subset \mathbb{R}^d$ be a bounded domain with Lipschitz boundary $\partial\Omega$ and let $0 < T < \infty$. We consider for the unknown $u = u(\mathbf{x} = (x_1, \dots, x_d)^T, t) : \Omega \times [0, T] \to \mathbb{R}$ an initial boundary value problem for nonlinear advection-diffusion equations given by

$$\partial_t u + \operatorname{div}(\mathbf{f}(u)) - \operatorname{div}(p(u)\nabla u) = 0 \quad \text{in} \quad \Omega \times (0, T), \tag{2.1}$$

$$u|_{t=0} = u_0 \quad \text{in} \quad \Omega, \tag{2.2}$$

$$u = 0 \quad \text{on} \quad \partial\Omega \times (0, T). \tag{2.3}$$

Here $p : \mathbb{R} \to (0, \infty)$ is a positive diffusion coefficient, $\mathbf{f} = (f_1, \dots, f_d)^T : \mathbb{R} \to \mathbb{R}^d$ is the advective flux, and $u_0 : \Omega \to \mathbb{R}$ is the initial data. Necessary requirements on these given functions will be summarized in Assumption 2.2 below. Working with a weak solution concept gives rise to define the function space $\mathcal{H} := H^1(0, T; H^{-1}(\Omega)) \cap L^2(0, T; H_0^1(\Omega))$.

DEFINITION 2.1 (weak solution to (2.1)–(2.3)). *A function $u \in \mathcal{H}$ is called a weak solution to problem (2.1)–(2.3) iff $u|_{t=0} = u_0$ a.e. in Ω and*

$$\int_0^T \langle \partial_t u,\ v\rangle + (p(u)\nabla u - \mathbf{f}(u),\ \nabla v)dt = 0 \tag{2.4}$$

for all $v \in L^2(0, T; H_0^1(\Omega))$.

Here, we denote by $\langle \cdot,\ \cdot \rangle$ the dual pairing between $H^{-1}(\Omega)$ and $H_0^1(\Omega)$, and by $(\cdot,\ \cdot)$ the inner product on $L^2(\Omega)$. The L^2-norm is denoted by $\|\cdot\|$ without further label, while norms of other spaces will be explicitly indicated in what follows. Note that for $u \in \mathcal{H}$, we also have $u \in C([0, T]; L^2(\Omega))$ by, e.g., [12, Ch. 5.9, Thm. 3], such that the equality $u|_{t=0} = u_0$ is well defined in $L^2(\Omega)$.

We apply a non-overlapping SWR algorithm to approximate the solution u of the problem (2.1)–(2.3) as proposed by Caetano et al. in [9] for the reaction-diffusion equation. For the analysis, we restrict ourselves to the two–sub-domain case; the generalization to multiple sub-domains is straightforward as long as the normal derivative of the weak solution to (2.1)–(2.3) exists as a trace on the sub-domain boundaries; cf. Theorem 4.1. More precisely, the domain Ω is partitioned into two non-overlapping sub-domains Ω_1 and Ω_2, such that both have Lipschitz boundaries $\partial\Omega_1$, $\partial\Omega_2$. We denote the common interface by $\Gamma := \partial\Omega_1 \cap \partial\Omega_2$, and by $\mathbf{n}_1$ and $\mathbf{n}_2$ the unit outward normal vectors to Ω_1 and Ω_2. The non-overlapping SWR algorithm is then given by iteratively solving for $k \in \mathbb{N}$ and $i = 1, 2$ the problems

$$\partial_t u_i^k + \operatorname{div}(\mathbf{f}(u_i^k)) - \operatorname{div}(p(u_i^k)\nabla u_i^k) = 0 \quad \text{in} \quad \Omega_i \times (0, T), \tag{2.5}$$

$$u_i^k|_{t=0} = u_0 \quad \text{in} \quad \Omega_i, \tag{2.6}$$

$$u_i^k = 0 \quad \text{on} \quad (\partial\Omega_i \backslash \Gamma) \times (0, T), \tag{2.7}$$

$$\mathfrak{B}_i(u_i^k) = \mathfrak{B}_i(u_{3-i}^{k-1}) \quad \text{on} \quad \Gamma \times (0,T). \tag{2.8}$$

Note that the index $3-i$ refers just to the other sub-domain, as $3-i = 2, 1$ for $i = 1, 2$. The differential transmission operators $\mathfrak{B}_i$ are chosen such that the continuity of the solution and of the normal flux across the interface is ensured in the limit. To this end, they are formulated as a linear combination of those, resulting in nonlinear Robin transmission conditions given for a fixed positive transmission parameter λ by

$$\mathfrak{B}_i(u) = (p(u)\nabla u - \mathbf{f}(u)) \cdot \mathbf{n}_i + \lambda u. \tag{2.9}$$

The iteration over $k \in \mathbb{N}$ is initialized by a given initial guess g_i of $\mathfrak{B}_i(u_{i-3}^0)$, i.e., (2.8) for $k = 1$ is replaced by $\mathfrak{B}_i(u_i^1) = g_i$ on $\Gamma \times (0,T)$. These transmission operators are the nonlinear counterparts of the linear ones, which have been studied, e.g., in [6, 9, 21, 25] as optimized approximations of the Dirichlet to Neumann operator; see [16] for an introduction and [28] for a comprehensive review. Before we proceed, let us note that the evaluation of the transmission operator can be expressed for $k > 1$ and $i = 1, 2$ by the shift relation

$$\begin{aligned} \mathfrak{B}_i(u_i^k) = \mathfrak{B}_i(u_{3-i}^{k-1}) &= \big(p(u_{3-i}^{k-1})\nabla u_{3-i}^{k-1} - \mathbf{f}(u_{3-i}^{k-1})\big) \cdot \mathbf{n}_i + \lambda u_{3-i}^{k-1} \\ &= 2\lambda u_{3-i}^{k-1} - \big(p(u_{3-i}^{k-1})\nabla u_{3-i}^{k-1} - \mathbf{f}(u_{3-i}^{k-1})\big) \cdot \mathbf{n}_{3-i} - \lambda u_{3-i}^{k-1} \\ &= 2\lambda u_{3-i}^{k-1} - \mathfrak{B}_{3-i}(u_{3-i}^{k-1}). \end{aligned} \tag{2.10}$$

For a weak definition of the iterative solutions of the SWR algorithm, we introduce the function spaces

$$X_i := \big\{ v \in H^1(\Omega_i) \,:\, v\big|_{\partial\Omega_i \setminus \Gamma} = 0 \big\}, \qquad \mathcal{H}_i := H^1(0,T;X_i^*) \cap L^2(0,T;X_i),$$

denoting by X_i^* the dual of X_i for $i \in \{1,2\}$. In our analysis, we make use of the following assumption on the problem and the SWR iteration data. Most notably we require (2.1) to be non-degenerate.

Assumption 2.2.

(i) The initial data u_0 satisfies $u_0 \in H_0^1(\Omega)$. The diffusion coefficient $p \in C_b^{0,1}(\mathbb{R})$ with Lipschitz constant $L_p > 0$ satisfies for some $\overline{p} > 0$ the condition $p(v) \geq \overline{p}$ for all $v \in \mathbb{R}$, and the flux function $\mathbf{f}$ is in $C_b^{0,1}(\mathbb{R}, \mathbb{R}^d)$, i.e., Lipschitz continuous with Lipschitz constant $L_f > 0$ and bounded.

(ii) The initial guesses of the transmission condition g_1 and g_2 are supposed to be in $L^2(0,T;L^2(\Gamma))$, and the transmission parameter λ is positive.

Note that the assumption applies for two-phase flow in porous media (in the non-degenerate regime), and also for the nonlinear viscous Burgers equation (cf. section 6), since the solution is bounded, so that, e.g., $\mathbf{f}(u) = \mathbf{v} \min(u^2, u_{\max}^2)$ and $p(u) = \max(u_{\min}, \min(u, u_{\max}))$ can be used to obtain bounded and Lipschitz-continuous functions. We use now (2.10) to avoid the evaluation of traces of gradients on Γ (see also [9, 25]) and are led to the following definition.

Definition 2.3 (weak solution to the SWR algorithm (2.5)–(2.8)). *Let Assumption* 2.2 *hold. For $i \in \{1,2\}$ and $k \in \mathbb{N}$ the functions $u_i^k \in \mathcal{H}_i$ are called a weak solution to the SWR algorithm* (2.5)–(2.9) *iff $u_i^k|_{t=0} = u_0$ a.e. in Ω_i and*

$$\int_0^T \big\langle \partial_t u_i^k,\, v \big\rangle + \big(p(u_i^k)\nabla u_i^k - \mathbf{f}(u_i^k),\, \nabla v\big)\, dt = \int_0^T \big(\mathfrak{B}_i^k - \lambda u_i^k,\, v\big)_\Gamma dt \tag{2.11}$$

for all $v \in L^2(0,T;X_i)$. *Here* $\mathfrak{B}_i^k \in L^2(0,T;L^2(\Gamma))$ *are given by* $\mathfrak{B}_i^1 = g_i$, *and iteratively for* $k > 1$ *through*

$$\mathfrak{B}_i^k = 2\lambda u_{3-i}^{k-1} - \mathfrak{B}_{3-i}^{k-1}. \tag{2.12}$$

Analogously as above for the entire domain, we denote here by $\langle \cdot, \cdot \rangle$ the dual pairing between X_i^* and X_i, by $(\cdot, \cdot)$ and $(\cdot, \cdot)_\Gamma$ the inner product on $L^2(\Omega_i)$ and $L^2(\Gamma)$, respectively. It will always be clear from the context whether $\|\cdot\|$ refers to either Ω_1, Ω_2, or the entire domain Ω. Furthermore, $\|\cdot\|_\Gamma$ denotes the $L^2(\Gamma)$-norm. Note again that for $u \in \mathcal{H}_i$, we have $u \in C([0,T];L^2(\Omega_i))$ by [12, Ch. 5.9, Thm. 3], such that $u|_{t=0} = u_0$ is well defined in $L^2(\Omega_i)$.

3. Existence of weak solutions and well-posedness of the SWR algorithm. In this section, we provide the existence and uniqueness results for the previously presented problems. For the original problem (2.1)–(2.3) existence and uniqueness of weak solutions in accordance with (2.1) has been proved by Alt and Luckhaus in [3].

LEMMA 3.1 (existence and uniqueness of a weak solution to (2.1)–(2.3)). *Let Assumption* 2.2 *hold, then there exists a unique weak solution* $u \in \mathcal{H}$ *to problem* (2.1)–(2.3), *which satisfies additionally* $\partial_t u \in L^2(0,T;L^2(\Omega))$.

Proof. Let $P(z) := \int_0^z p(y)dy$, so we have $P, P^{-1} \in C^{1,1}(\mathbb{R})$ by Assumption 2.2. We define the Kirchhoff transformed solution $w := P(u)$. The function u is a weak solution to (2.1)–(2.3) iff w satisfies $w|_{t=0} = w_0 := P(u_0)$ a.e. in Ω and

$$\int_0^T \left\langle \partial_t P^{-1}(w),\ v \right\rangle + \big(\nabla w - \mathbf{f}(P^{-1}(w)),\ \nabla v\big) dt = 0$$

for all $v \in L^2(0,T;H_0^1(\Omega))$. The existence of a unique weak solution $w \in \mathcal{H}$ follows by [3, Thms. 1.7, 2.4], while $\partial_t u = \partial_t P^{-1}(w) \in L^2(0,T;L^2(\Omega))$ follows by [3, Thm. 2.3]. Hence, we obtain the unique weak solution u by the inverse Kirchhoff transform. ∎

In the next step we provide a well-posedness result for the SWR algorithm (2.5)–(2.8). The proof relies on compactness arguments as in [3] but requires iteration-independent a priori estimates and a generalization to account for the transmission conditions in the weak form (2.11). We start with the construction of approximate solutions in time. Taking the limit, we will verify the existence of a weak solution in the sense of Definition 2.3.

DEFINITION 3.2 (time-discrete problem). *Let* $\Delta t > 0$, *and* $\mathfrak{D}_i \in L^2(0,T;L^2(\Gamma))$ *for* $i \in \{1,2\}$ *be given. For* $n \in 0,\dots,T/\Delta t$ *and* $i \in \{1,2\}$ *the functions* $u_{n,i} \in X_i$ *are called a solution to the time-discrete problem iff* $u_{0,i} = u_0$ *in* X_i *and*

$$\left(\frac{u_{n,i} - u_{n-1,i}}{\Delta t},\ v\right) + (p(u_{n,i})\nabla u_{n,i} - \mathbf{f}(u_{n,i}),\ \nabla v) = (\mathfrak{D}_{n,i} - \lambda u_{n,i},\ v)_\Gamma \tag{3.1}$$

for all $v \in X_i$, *where* $\mathfrak{D}_{n,i} = \frac{1}{\Delta t}\int_{(n-1)\Delta t}^{n\Delta t} \mathfrak{D}_i(s)ds$.

LEMMA 3.3. *Let Assumption* 2.2 *hold. For* Δt *small enough,* $n \in 0,\dots,T/\Delta t$, *and* $i \in \{1,2\}$, *there exist unique* $u_{n,i} \in X_i$ *solving the time-discrete problem from Definition* 3.2.

Proof. The $u_{n,i}$ can be determined inductively for n as solutions of nonlinear elliptic problems. Again, let $P(z) := \int_0^z p(y)dy$, so we have $P, P^{-1} \in C^{1,1}(\mathbb{R})$ by

Assumption 2.2. We define the Kirchhoff transformed solution $w_{n,i} := P(u_{n,i}) \in X_i$. The function $u_{n,i}$ is a solution to (3.1) iff $w_{n,i}$ satisfies

$$\begin{aligned} &\left(\frac{P^{-1}(w_{n,i}) - P^{-1}(w_{n-1,i})}{\Delta t},\ v\right) + \big(\nabla w_{n,i} - \mathbf{f}(P^{-1}(w_{n,i})),\ \nabla v\big) \\ &\quad = \big(\mathfrak{D}_{n,i} - \lambda P^{-1}(w_{n,i}),\ v\big)_\Gamma \end{aligned} \tag{3.2}$$

for all $v \in X_i$. One can write (3.2) in the functional form $a(w_{n,i}, v) = b(v)$ using the bounded linear operator $b : X_i \to \mathbb{R}$ defined by

$$b(v) := \frac{1}{\Delta t}\big(P^{-1}(w_{n-1,i}),\ v\big) + (\mathfrak{D}_{n,i},\ v)_\Gamma$$

and the nonlinear operator $a : X_i \times X_i \to \mathbb{R}$ given by

$$a(w,\, v) := \frac{1}{\Delta t}\big(P^{-1}(w),\ v\big) + \big(\nabla w - \mathbf{f}(P^{-1}(w)),\ \nabla v\big) + \lambda\big(P^{-1}(w),\ v\big)_\Gamma.$$

Clearly, $a_w := a(w, \cdot)$ is a bounded linear operator for each $w \in X_i$. Furthermore, since $\frac{1}{\|p\|_{C_b^0}} \le (P^{-1})' \le \frac{1}{\overline{p}}$, we have with the Cauchy–Schwarz and the Young inequalities

$$\begin{aligned} a(u, u-v) - a(v, u-v) &\ge \frac{1}{\Delta t\|p\|_{C_b^0}}\|u-v\|^2 + \|\nabla(u-v)\|^2 \\ &\quad - \frac{L_f}{\overline{p}}\|u-v\|\,\|\nabla(u-v)\| + \frac{\lambda}{\|p\|_{C_b^0}}\|u-v\|_\Gamma^2 \\ &\ge \min\left\{\frac{1}{\Delta t\|p\|_{C_b^0}} - \frac{L_f}{2\overline{p}}, \frac{1}{2}\right\}\|u-v\|_{X_i}^2, \\ |a(u,v) - a(w,v)| &\le \frac{1}{\Delta t\overline{p}}\|u-w\|\,\|v\| + \|\nabla(u-w)\|\,\|\nabla v\| \\ &\quad + \frac{L_f}{\overline{p}}\|u-w\|\,\|\nabla v\| + \frac{\lambda}{\overline{p}}\|u-w\|_\Gamma\|v\|_\Gamma \\ &\le C\|u-w\|_{X_i}\|v\|_{X_i}. \end{aligned}$$

For $\Delta t < \frac{2\overline{p}}{L_f\|p\|_{C_b^0}}$, the nonlinear Lax–Milgram theorem [53, Thm. 2.H, pp. 174–175] provides the existence and uniqueness of the solutions $w_{n,i} \in X_i$ for all n, and thus the existence and uniqueness of the solutions $u_{n,i} \in X_i$ of (3.1). ∎

Having established the existence for the time-discrete problems, we proceed with investigating the SWR algorithm. To this end, we start with some a priori estimates.

LEMMA 3.4. *Let Assumption 2.2 hold. The solutions $u_{n,i}$ of the time-discrete problem from Definition 3.2 satisfy*

$$\begin{aligned} \max_{n\in\{1,\dots,T/\Delta t\}}\|u_{n,i}\|^2 + \sum_{n=1}^{T/\Delta t}\Delta t\|\nabla u_{n,i}\|^2 + \sum_{n=1}^{T/\Delta t}\Delta t\|u_{n,i}\|_\Gamma^2 &\le C\left(1 + \|\mathfrak{D}_i\|^2_{L^2(0,T;L^2(\Gamma))}\right), \\ \sum_{n=1}^{T/\Delta t}\Delta t\Big\|\frac{u_{n,i}-u_{n-1,i}}{\Delta t}\Big\|_{X_i^*}^2 &\le C\left(1 + \|\mathfrak{D}_i\|^2_{L^2(0,T;L^2(\Gamma))}\right), \end{aligned}$$

with some constant $C > 0$ independent of Δt and $\mathfrak{D}_i$.

Proof. Let $v = u_{n,i}$ in (3.1). Then, we obtain

$$\begin{aligned}&\frac{1}{\Delta t}\|u_{n,i}\|^2 + \overline{p}\|\nabla u_{n,i}\|^2 + \lambda\|u_{n,i}\|_\Gamma^2\\ &\quad\le \frac{1}{\Delta t}(u_{n-1,i},\ u_{n,i}) + (\mathbf{f}(u_{n,i}),\ \nabla u_{n,i}) + (\mathfrak{D}_i^n,\ u_{n,i})_\Gamma,\end{aligned}$$

and we have by the Cauchy–Schwarz and the Young inequalities

$$\frac{1}{\Delta t}\|u_{n,i}\|^2 + \overline{p}\|\nabla u_{n,i}\|^2 + \lambda\|u_{n,i}\|_\Gamma^2 \le \frac{1}{\Delta t}\|u_{n-1,i}\|^2 + \frac{1}{\overline{p}}\|\mathbf{f}\|_{C_b^0}^2|\Omega_i| + \frac{1}{\lambda}\|\mathfrak{D}_{n,i}\|_\Gamma^2.$$

Multiplication by Δt and summation over n from 1 to some $N \in \mathbb{N}$ finally yields

$$\begin{aligned}&\|u_{N,i}\|^2 + \overline{p}\sum_{n=1}^N \Delta t\|\nabla u_{n,i}\|^2 + \lambda\sum_{n=1}^N \Delta t\|u_{n,i}\|_\Gamma^2\\ &\quad\le \|u_{0,i}\|^2 + \frac{1}{\overline{p}}\|\mathbf{f}\|_{C_b^0}^2|\Omega_i|T + \frac{1}{\lambda}\|\mathfrak{D}_i\|_{L^2(0,T;L^2(\Gamma))}^2.\end{aligned}$$

This implies the first a priori estimate. Now consider an arbitrary $v \in X_i$ in (3.1); then we obtain with the Cauchy–Schwarz inequality and the trace theorem

$$\begin{aligned}\left|\left(\frac{u_{n,i}-u_{n-1,i}}{\Delta t},\ v\right)\right| &\le \big(\overline{p}\|\nabla u_{n,i}\| + \|\mathbf{f}(u_{n,i})\|\big)\|\nabla v\| + \big(\|\mathfrak{D}_{n,i}\|_\Gamma + \lambda\|u_{n,i}\|_\Gamma\big)\|v\|_\Gamma\\ &\le C_1\big(\|\nabla u_{n,i}\| + \|\mathbf{f}(u_{n,i})\| + \|\mathfrak{D}_{n,i}\|_\Gamma + \|u_{n,i}\|_\Gamma\big)\|v\|_{X_i}.\end{aligned}$$

Dividing by $\|v\|_{X_i}$ for $v \ne 0$ and taking the square, we obtain

$$\left\|\frac{u_{n,i}-u_{n-1,i}}{\Delta t}\right\|_{X_i^*}^2 \le C_2\left(\|\nabla u_{n,i}\|^2 + \|\mathbf{f}\|_{C_b^0}^2|\Omega_i| + \|\mathfrak{D}_{n,i}\|_\Gamma^2 + \|u_{n,i}\|_\Gamma^2\right).$$

Multiplication by Δt and summation with respect to $n = 1, \dots, N$ lead to

$$\begin{aligned}&\sum_{n=1}^N \Delta t\left\|\frac{u_{n,i}-u_{n-1,i}}{\Delta t}\right\|_{X_i^*}^2\\ &\quad\le C_2\sum_{n=1}^N \Delta t\left(\|\nabla u_{n,i}\|^2 + \|\mathbf{f}\|_{C_b^0}^2|\Omega_i| + \|\mathfrak{D}_{n,i}\|_\Gamma^2 + \|u_{n,i}\|_\Gamma^2\right).\end{aligned}$$

Using the first a priori estimate concludes the proof. ∎

Based on the a priori estimates for the approximate solutions, we take the limit $\Delta t \to 0$ in (3.1) to conclude the existence of a weak solution of single SWR iterates in the sense of Definition 2.3. The arguments are similar to the uniqueness proof of [3, Thm. 1.7].

THEOREM 3.5 (existence of weak solutions to (2.5)–(2.8)). *Let Assumption 2.2 hold. Then, for $i \in \{1,2\}$ and all $k \in \mathbb{N}$ there exists a weak solution $u_i^k \in \mathcal{H}_i$ to the SWR algorithm (2.5)–(2.8) that satisfies the estimate*

$$\begin{aligned}&\|u_i^k\|_{L^\infty(0,T;L^2(\Omega_i))}^2 + \|u_i^k\|_{L^2(0,T;X_i)}^2 + \|\partial_t u_i^k\|_{L^2(0,T;X_i^*)}^2 + \|u_i^k\|_{L^2(0,T;L^2(\Gamma))}^2\\ &\quad\le C\left(1 + \|\mathfrak{B}_i^k\|_{L^2(0,T;L^2(\Gamma))}^2\right),\end{aligned} \tag{3.3}$$

where $C \geq 0$ depends on $|\Omega_i|$, T, λ, $\overline{p}$, $\|p\|_{C_b^0}$, $\|\mathbf{f}\|_{C_b^0}$, and $\|u_0\|_{H^1(\Omega_i)}$.

Proof. The time-discrete problem from Definition 3.2 with $\mathfrak{D}_i := \mathfrak{B}_i^k$ given by (2.12) has unique solutions $u_{n,i}^k \in X_i$ by Lemma 3.3, which satisfy the a priori estimates in Lemma 3.4. Let $u_{\Delta t,i}^k : \Omega_i \times [0,T] \to \mathbb{R}$ be the piecewise linear interpolation in time of the functions $u_{0,i}^k, \dots, u_{T/\Delta t,i}^k$. Then we have

$$\begin{aligned}\int_0^T \left\|u_{\Delta t,i}^k\right\|^2 dt &= \sum_{n=1}^{T/\Delta t} \int_{(n-1)\Delta t}^{n\Delta t} \left\| u_{n-1,i}^k + \frac{t-(n-1)\Delta t}{\Delta t}(u_{n,i}^k - u_{n-1,i}^k)\right\|^2 dt \\ &\leq 2\sum_{n=1}^{T/\Delta t} \int_{(n-1)\Delta t}^{n\Delta t} \left\|u_{n-1,i}^k\right\|^2 + \left\|u_{n,i}^k\right\|^2 dt \\ &\leq 2C\left(1 + \left\|\mathfrak{B}_i^k\right\|_{L^2(0,T;L^2(\Gamma))}^2\right),\end{aligned}$$

and similarly

$$\begin{aligned}\int_0^T \left\|\nabla u_{\Delta t,i}^k\right\|^2 dt &\leq 2C\left(1 + \left\|\mathfrak{B}_i^k\right\|_{L^2(0,T;L^2(\Gamma))}^2\right), \\ \int_0^T \left\|\partial_t u_{\Delta t,i}^k\right\|_{X_i^*}^2 dt &= \sum_{n=1}^{T/\Delta t} \int_{(n-1)\Delta t}^{n\Delta t} \left\|\frac{u_{n,i}^k - u_{n-1,i}^k}{\Delta t}\right\|_{X_i^*}^2 dt \\ &\leq C\left(1 + \left\|\mathfrak{B}_i^k\right\|_{L^2(0,T;L^2(\Gamma))}^2\right).\end{aligned}$$

Therefore, the family $(u_{\Delta t,i}^k)_{\Delta t>0}$ is uniformly bounded in $\mathcal{H}_i$, so it has a weakly converging subsequence with limit $u_i^k \in \mathcal{H}_i$. Using the compact embedding of $\mathcal{H}_i$ into $L^2(0,T;L^2(\Omega_i))$ (the Aubin–Lions lemma), we have that $u_{\Delta t,i}^k$ converges strongly to u_i^k in $L^2(0,T;L^2(\Omega_i))$. We use now the general principle that the strong convergence of the piecewise linear time-interpolation in $L^2(0,T;L^2(\Omega))$ implies the same convergence and limit for the piecewise constant interpolation in time; see, e.g., [40, Lemma 3.2]. Thus, we conclude that the piecewise constant interpolation in time, defined by $\overline{u_{\Delta t,i}^k}(t) := u_{n,i}^k$ for $t \in ((n-1)\Delta t, n\Delta t]$, also converges strongly in $L^2(0,T;L^2(\Omega))$.

Further, observe that $p(\overline{u_{\Delta t,i}^k})\nabla\overline{u_{\Delta t,i}^k}$ is bounded in $[L^2(0,T;L^2(\Omega_i))]^d$; therefore it has a weak limit ξ_i^k in this space. To identify this limit, we take arbitrary $v \in L^2(0,T;X_i \cap C^1(\overline{\Omega_i}))$ as test functions. Then, we obtain

$$\begin{aligned}&\int_0^T \left(p(\overline{u_{\Delta t,i}^k})\nabla\overline{u_{\Delta t,i}^k} - p(u_i^k)\nabla u_i^k,\ \nabla v\right) dt \\ &\quad= \int_0^T \left(\left(p(\overline{u_{\Delta t,i}^k}) - p(u_i^k)\right)\nabla\overline{u_{\Delta t,i}^k},\ \nabla v\right) + \left(p(u_i^k)\left(\nabla\overline{u_{\Delta t,i}^k} - \nabla u_i^k\right),\ \nabla v\right) dt \\ &\quad= \int_0^T \left(\nabla\overline{u_{\Delta t,i}^k},\ \left(p(\overline{u_{\Delta t,i}^k}) - p(u_i^k)\right)\nabla v\right) + \left(\nabla\overline{u_{\Delta t,i}^k} - \nabla u_i^k,\ p(u_i^k)\nabla v\right) dt.\end{aligned}$$

Since $p(\overline{u_{\Delta t,i}^k})$ converges strongly, and $\nabla\overline{u_{\Delta t,i}^k}$ converges weakly in $L^2(0,T;L^2(\Omega_i))$ (analogously to $u_{\Delta t,i}^k$), and ∇v is bounded, the terms on the right-hand side converge to zero. By the uniqueness of the limit, we have then $\xi_i^k = p(u_i^k)\nabla u_i^k$.

From (3.1), we know

$$\int_0^T \langle \partial_t u_{\Delta t,i}^k,\ v\rangle + \left(p(\overline{u_{\Delta t,i}^k})\nabla\overline{u_{\Delta t,i}^k} - \mathbf{f}(\overline{u_{\Delta t,i}^k}),\ \nabla v\right) dt = \int_0^T \left(\overline{\mathfrak{B}_i^k} - \lambda\overline{u_{\Delta t,i}^k},\ v\right)_\Gamma dt$$

for all $v \in L^2(0,T;X_i)$. The function $\overline{\mathfrak{B}_i^k}$ is iteratively defined by $\overline{\mathfrak{B}_i^k} = 2\lambda\overline{u_{\Delta t,3-i}^{k-1}} - \overline{\mathfrak{B}_{3-i}^{k-1}}$. Due to the strong and weak convergence of $u_{\Delta t,i}^k$ and $\overline{u_{\Delta t,i}^k}$, we can consider a sequence $\Delta t \to 0$ and pass to the limit, which shows that u_i^k is a weak solution to the SWR algorithm (2.5)–(2.8). Thus, we can iteratively obtain weak solutions $u_i^k \in \mathcal{H}_i$ for $i = 1, 2$ and $k \in \mathbb{N}$, such that the estimate (3.3) is satisfied. ∎

The existence of a solution to the SWR algorithm is used in the next theorem to prove the uniqueness of the solutions for the SWR iterations under an additional regularity assumption.

THEOREM 3.6 (uniqueness of the SWR iteration). *Let Assumption* 2.2 *hold. If a sequence of weak solutions* $(u_1^k, u_2^k)_{k\in\mathbb{N}}$ *to the SWR algorithm* (2.5)–(2.9) *satisfies* $\partial_t u_i^k \in L^2(0,T;L^2(\Omega_i))$ *for* $i \in \{1,2\}$ *and all* $k \in \mathbb{N}$, *it is unique.*

Remark 3.7. The regularity assumption $\partial_t u_i^k \in L^2(0,T;L^2(\Omega_i))$ amounts to the maximal-regularity property for parabolic equations, i.e., the required regularity when dealing with strong solutions. In [51] maximal regularity is proven for a wide class of quasilinear parabolic equations including equations of type (2.3). The results apply if $\mathbf{f}$ and the diffusion coefficient satisfy Assumption 2.2 and if the domain boundary is $C^{1,1}$-regular. Thus, Theorem 4.1 holds under these general conditions, which are satisfied if, e.g., $d = 1$ holds, or if $\partial\Omega_1$ and $\partial\Omega_2$ can be chosen to be smooth. The $C^{1,1}$-regularity of the boundaries can be guaranteed if one of the sub-domains is immersed into the other one such that $\Gamma = \partial\Omega_1 \cap \partial\Omega_2$ does not intersect with $\partial\Omega$. For the case $\Gamma \cap \partial\Omega \neq \emptyset$ which excludes $C^{1,1}$-regularity for Ω_1 and Ω_2, there are to the best of our knowledge only a few general results, none of which cover (2.3) completely. The recent contribution [4] for linear evolution equations with variable coefficients establishes maximal regularity for transversal intersections of Γ with the boundary $\partial\Omega$.

Proof of Theorem 3.6. Assume that there is another sequence of weak solutions $(\tilde{u}_1^k, \tilde{u}_2^k)_{k\in\mathbb{N}}$. Then there exists an $i \in \{1,2\}$ and a $k \in \mathbb{N}$ minimal, such that $u_i^k \neq \tilde{u}_i^k$ and $\mathfrak{B}_i^k = \tilde{\mathfrak{B}}_i^k$. Let $\psi_\delta(z) := \max(0, \min(1, z/\delta))$. We follow the proof of Theorem 2.2 in [3] and consider the difference of the equations (2.11) for both solutions with the choice $v = \psi_\delta(u_i^k - \tilde{u}_i^k)\chi_{(0,\tau)}$ for $\tau \in (0,T]$. This yields

$$\int_0^\tau \int_{\Omega_i} \partial_t(u_i^k - \tilde{u}_i^k)\psi_\delta(u_i^k - \tilde{u}_i^k)dx + \big(p(u_i^k)\nabla u_i^k - p(\tilde{u}_i^k)\nabla\tilde{u}_i^k,\ \nabla\psi_\delta(u_i^k - \tilde{u}_i^k)\big)dt + \int_0^\tau \big(u_i^k - \tilde{u}_i^k,\ \psi_\delta(u_i^k - \tilde{u}_i^k)\big)_\Gamma dt = \int_0^\tau \big(\mathbf{f}(u_i^k) - \mathbf{f}(\tilde{u}_i^k),\ \nabla\psi_\delta(u_i^k - \tilde{u}_i^k)\big).$$

By the identity $p(u_i^k)\nabla u_i^k - p(\tilde{u}_i^k)\nabla\tilde{u}_i^k = p(\tilde{u}_i^k)\nabla(u_i^k - \tilde{u}_i^k) + (p(u_i^k) - p(\tilde{u}_i^k))\nabla u_i^k$, the Cauchy–Schwarz inequality, and the Young inequality, we get

$$\begin{aligned}
&\int_0^\tau \int_{\Omega_i} \partial_t(u_i^k - \tilde{u}_i^k)\psi_\delta(u_i^k - \tilde{u}_i^k)dx + \frac{\delta\overline{p}}{2}\big\|\nabla\psi_\delta(u_i^k - \tilde{u}_i^k)\big\|^2 dt \\
&\quad\le \int_0^\tau \frac{L_p^2}{\delta\overline{p}}\big\|\chi_{\{0\le u_i^k - \tilde{u}_i^k \le\delta\}}|u_i^k - \tilde{u}_i^k||\nabla u_i^k|\big\|^2 + \frac{L_f^2}{\delta\overline{p}}\big\|\chi_{\{0\le u_i^k - \tilde{u}_i^k\le\delta\}}(u_i^k - \tilde{u}_i^k)\big\|^2 dt \\
&\quad\le \int_0^\tau \frac{\delta L_p^2}{\overline{p}}\big\|\nabla u_i^k\big\|^2 + \frac{\delta L_f^2|\Omega_i|}{\overline{p}}dt.
\end{aligned}$$

For $\delta \to 0$, the right-hand side tends to zero and the first term on the left-hand side converges for almost all $\tau \in (0,T)$ to

$$\int_0^\tau \int_{\Omega_i} \partial_t (u_i^k - \tilde{u}_i^k) \chi_{\{u_i^k \geq \tilde{u}_i^k\}} dx dt = \int_0^\tau \int_{\Omega_i} \partial_t \max(u_i^k - \tilde{u}_i^k, 0) dx dt$$
$$= \int_{\Omega_i} \max(u_i^k(\tau) - \tilde{u}_i^k(\tau), 0) dx \geq 0.$$

Interchanging the roles of u_i^k and $\tilde{u}_i^k$, we obtain

$$0 = \int_{\Omega_i} \left| u_i^k(\tau) - \tilde{u}_i^k(\tau) \right| dx$$

for almost all τ and hence $u_i^k = \tilde{u}_i^k$ almost everywhere. ∎

4. Convergence of the non-overlapping SWR algorithm. We now prove that the weak solutions of the non-overlapping SWR algorithm (2.5)–(2.9) converge to the weak solution of the entire domain (mono-domain) formulation (2.1)–(2.3), and hence this method is applicable to nonlinear advection-diffusion equations. We use the conceptual idea of Caetano et al. in [9] for a semi-linear reaction diffusion equation $\partial_t u - \nu \Delta u = r(u)$ with some source function $r(u)$, but with substantial differences: the proof in [9] requires a priori estimates in higher-order Sobolev spaces and leads in a first step only to a result locally in time. Here we exploit the low-order ansatz for weak solutions from [3], which enables us to deduce directly a global error bound, which extends the similar result for stationary linear advection-diffusion equations in [44, Thm. 4.5] to nonlinear advection-diffusion equations.

THEOREM 4.1 (convergence of the SWR iteration). *Let Assumption* 2.2 *be satisfied. By Theorem* 3.5, *the SWR algorithm defined by* (2.5)–(2.9), *initialized with the guesses* $g_1, g_2 \in L^2(0,T;L^2(\Gamma))$, *defines a sequence of weak solutions* $(u_1^k, u_2^k) \in \mathcal{H}_1 \times \mathcal{H}_2$, *which is unique if* $\partial_t u_i^k \in L^2(0,T;L^2(\Omega_i))$ *for* $i \in \{1,2\}$ *and all* $k \in \mathbb{N}$ *by Theorem* 3.6.

If the unique weak solution u *of the original problem* (2.1)–(2.3) *satisfies* $\nabla u \in L^2(0,T;L^\infty(\Omega))$ *and* $p(u)\nabla u \cdot \mathbf{n}_i \in L^2(0,T;L^2(\Gamma))$, *then* $(u_1^k, u_2^k)_{k\in\mathbb{N}}$ *converges to* $(u|_{\Omega_1}, u|_{\Omega_2})$ *in* $(L^\infty(0,T;L^2(\Omega_i)) \cap L^2(0,T;X_i))_{i=1,2}$ *as* $k \to \infty$.

Note that the regularity assumptions $p(u)\nabla u \cdot \mathbf{n}_i \in L^2(0,T;L^2(\Gamma))$ and $\nabla u \in L^2(0,T;L^\infty(\Omega))$ can be shown, e.g., by the following regularity results in case of more regularity of the domain and of the parameter functions.

LEMMA 4.2 (improved regularity of the solution to (2.1)–(2.3)). *Let Assumption* 2.2 *hold. If we additionally have* $\partial\Omega \in C^{1,1}$ *or* Ω *convex and* $\mathbf{f} \in C_b^1(\mathbb{R},\mathbb{R}^d)$, *then the solution* u *to problem* (2.1)–(2.3) *is in* $L^2(0,T;H^2(\Omega)) \cap C([0,T];H^1(\Omega))$.

Proof. Since $\mathbf{f}'$ is continuous and bounded, $\mathbf{f}'(u)\cdot\nabla u$ is Lebesgue measurable and in $L^2(0,T;L^2(\Omega))$. Thus, integration by parts in (2.4) yields

$$\int_0^T (\nabla w,\ \nabla v) dt := \int_0^T (p(u)\nabla u,\ \nabla v) dt$$
$$= \int_0^T (\partial_t u + \mathbf{f}'(u)\cdot\nabla u,\ v) dt =: \int_0^T (g,\ v) dt$$

for all $v \in L^2(0,T;H_0^1(\Omega))$, where $g \in L^2(0,T;L^2(\Omega))$. Since time is only a parameter, we obtain by the regularity theory in [32] that $w = P(u) \in L^2(0,T;H^2(\Omega))$. As $p = P'$

is bounded from below by $\overline{p} > 0$, this yields $\nabla u \in L^2(0,T;H^1(\Omega))$. Together with $\partial_t u \in L^2(0,T;L^2(\Omega))$, we obtain $u \in C([0,T];H^1(\Omega))$ by [12, Ch. 5.9, Thm. 4]. ∎

LEMMA 4.3 (classical solution to (2.1)–(2.3)). *Let Assumption 2.2 hold, and additionally assume $\partial\Omega \in C^2$, $p \in C_b^{1,\alpha}(\mathbb{R})$, and $\mathbf{f} \in C_b^{1,\alpha}(\mathbb{R},\mathbb{R}^d)$ for some $\alpha > 0$. If the initial data u_0 is in $C^{0,1}(\Omega)$, then there exists a unique solution $u \in C^{0,\alpha/2}([0,T]\times\overline{\Omega}) \cap C^1((0,T);C^0(\Omega)) \cap C^0((0,T);C^2(\Omega))$ to problem (2.1)–(2.3).*

Proof. By direct application of [38, Chp. V, Thm. 6.2]. ∎

Proof of Theorem 4.1. For each $k \in \mathbb{N}$ and $i \in \{1,2\}$, we define the errors $e_i^k := u_i^k - u|_{\Omega_i} \in \mathcal{H}_i$. Note that $\partial_t u \in L^2(0,T;L^2(\Omega))$ by regularity, such that $\langle \partial_t u,\ \cdot\rangle$ on Ω equals the sum of the corresponding dual pairings on Ω_1 and Ω_2. Thus, the errors satisfy on the sub-domains the initial boundary value problems

$$\begin{aligned}\int_0^T \big\langle \partial_t e_i^k,\ v\big\rangle + \big(p(u_i^k)\nabla e_i^k + (p(u_i^k)-p(u))\nabla u - \mathbf{f}(u_i^k) + \mathbf{f}(u),\ \nabla v\big)dt \\ = \int_0^T \Big(\mathfrak{B}_i^{k,\mathrm{err}} - \lambda e_i^k,\ v\Big)_\Gamma dt\end{aligned} \tag{4.1}$$

for all $v \in L^2(0,T;X_i)$, together with the initial data $e_i^k|_{t=0} = 0$ in $L^2(\Omega_i)$ and the error transmission operator defined due to the assumptions and (2.9) by

$$\mathfrak{B}_i^{k,\mathrm{err}} := \mathfrak{B}_i^k - \big(p(u)\nabla u - \mathbf{f}(u)\big)\cdot\mathbf{n}_i - \lambda u \qquad \text{on } \Gamma\times(0,T). \tag{4.2}$$

Choosing $v = e_i^k \chi_{(0,\tau)}$ for $\tau \in (0,T]$ in (4.1) and applying the Cauchy–Schwarz inequality yields

$$\begin{aligned}&\frac{1}{2}\big\|e_i^k(\tau)\big\|^2 + \int_0^\tau \overline{p}\big\|\nabla e_i^k\big\|^2 - \Big(\big\|(p(u_i^k)-p(u))\nabla u\big\| + \big\|\mathbf{f}(u_i^k)+\mathbf{f}(u)\big\|\Big)\big\|\nabla e_i^k\big\|dt \\ &\quad\le \int_0^\tau \Big(\mathfrak{B}_i^{k,\mathrm{err}} - \lambda e_i^k,\ e_i^k\Big)_\Gamma dt.\end{aligned}$$

Using $p, \mathbf{f} \in C_b^{0,1}$ and the Young inequality, we obtain

$$\begin{aligned}&\frac{1}{2}\big\|e_i^k(\tau)\big\|^2 + \overline{p}\Big(1-\frac{1}{2}\Big)\int_0^\tau \big\|\nabla e_i^k\big\|^2 dt \\ &\quad\le \int_0^\tau \Big(\mathfrak{B}_i^{k,\mathrm{err}} - \lambda e_i^k,\ e_i^k\Big)_\Gamma dt + \int_0^\tau \left(\frac{L_p^2}{\overline{p}}\big\|\nabla u\big\|_{L^\infty(\Omega_i)}^2 + \frac{L_f^2}{\overline{p}}\right)\big\|e_i^k\big\|^2 dt.\end{aligned}$$

Next, we replace the transmission term using the identity $\mathfrak{B}_i^{k,\mathrm{err}} = 2\lambda e_{3-i}^{k-1} - \mathfrak{B}_{3-i}^{k-1,\mathrm{err}}$ (see (2.10) and (2.12)), yielding

$$\big\|\mathfrak{B}_i^{k,\mathrm{err}}\big\|_\Gamma^2 = \big\|\mathfrak{B}_{3-i}^{k-1,\mathrm{err}}\big\|_\Gamma^2 - 4\lambda\Big(\mathfrak{B}_{3-i}^{k-1,\mathrm{err}},\ e_i^k\Big)_\Gamma + 4\lambda^2\big\|e_{3-i}^{k-1}\big\|_\Gamma^2,$$

such that we have by shifting i and k

$$\Big(\mathfrak{B}_i^{k,\mathrm{err}} - \lambda e_i^k,\ e_i^k\Big)_\Gamma = \frac{1}{4\lambda}\left(\big\|\mathfrak{B}_i^{k,\mathrm{err}}\big\|_\Gamma^2 - \big\|\mathfrak{B}_{3-i}^{k+1,\mathrm{err}}\big\|_\Gamma^2\right).$$

Hence, we get

$$\begin{aligned}&\big\|e_i^k(\tau)\big\|^2 + \overline{p}\int_0^\tau \big\|\nabla e_i^k\big\|^2 dt \\ &\quad\le \frac{1}{2\lambda}\int_0^\tau \big\|\mathfrak{B}_i^{k,\mathrm{err}}\big\|_\Gamma^2 - \big\|\mathfrak{B}_{3-i}^{k+1,\mathrm{err}}\big\|_\Gamma^2 dt + \int_0^\tau C_E(t)\big\|e_i^k\big\|^2 dt,\end{aligned} \tag{4.3}$$

where

$$C_E(t) = \frac{2L_p^2}{\overline{p}} \left\| \nabla u(t) \right\|^2_{L^\infty(\Omega_i)} + \frac{2L_f^2}{\overline{p}} > 0.$$

Adding terms up to step $K \in \mathbb{N}$ for both sub-domains, we define

$$\mathfrak{E}^K(\tau) := \sum_{k=1}^{K} \sum_{i=1}^{2} \left\| e_i^k(\tau) \right\|^2, \qquad \mathfrak{F}^K(\tau) := \overline{p} \sum_{k=1}^{K} \sum_{i=1}^{2} \int_0^\tau \left\| \nabla e_i^k \right\|^2 dt,$$

$$\mathfrak{G}^K(\tau) := \frac{1}{2\lambda} \sum_{i=1}^{2} \int_0^\tau \left\| \mathfrak{B}_i^{K,\mathrm{err}} \right\|^2_\Gamma dt.$$

Summing (4.3) over $k = 1, \dots, K$ and $i = 1, 2$, we obtain the inequality

$$\mathfrak{E}^K(\tau) + \mathfrak{F}^K(\tau) + \mathfrak{G}^{K+1}(\tau) \leq \mathfrak{G}^1(\tau) + \int_0^\tau C_E(t) \mathfrak{E}^K(t) dt.$$

Note that $C_E \in L^1(0,T)$ by assumption, and $\mathfrak{E}^K \in C([0,T])$, so that we conclude by Gronwall's lemma

$$\mathfrak{E}^K(\tau) \leq \mathfrak{G}^1(\tau) + \int_0^\tau \mathfrak{G}^1(t) C_E(t) \exp\left(\int_t^\tau C_E(s) ds \right) dt =: C(t) < \infty, \tag{4.4}$$

$$\mathfrak{F}^K(\tau) \leq \mathfrak{G}^1(\tau) + \int_0^\tau C_E(t) C(t) dt < \infty. \tag{4.5}$$

Since the right-hand side of the estimates (4.4) and (4.5) are independent of K, the sequences $(\mathfrak{E}^k)_{k\in\mathbb{N}}$ and $(\mathfrak{F}^k)_{k\in\mathbb{N}}$ are uniformly bounded in $L^\infty(0,T)$. Therefore, u_i^k converges to $u|_{\Omega_i}$ in $L^\infty(0,T; L^2(\Omega_i)) \cap L^2(0,T; X_i)$. ∎

5. Numerical discretization for two-dimensional domains. To implement the SWR algorithm we suggest discretizing the equations by a finite volume method. This allows us in particular to enforce the transmission conditions quite naturally via numerical fluxes across the interface.

5.1. The general finite volume method. We consider for $d = 2$ the bounded domain $\Omega = (-1,1)^2$. For the SWR algorithm, the (mono-)domain Ω is divided at $\Gamma = \{0\} \times [-1,1]$ into the two (sub-)domains $\Omega_1 = (-1,0) \times (-1,1)$ and $\Omega_2 = (0,1) \times (-1,1)$. For all domains $\omega \in \{\Omega, \Omega_1, \Omega_2\}$ we use as discretization a first-order finite volume method on a conforming structured mesh $\mathcal{T}_{\omega,\Delta x}$ of equilateral triangles; the mesh parameter $\Delta x > 0$ denotes the length of the edges. For some $\mathcal{T} \in \mathcal{T}_{\omega,\Delta x}$ we denote by $\mathcal{S}(\mathcal{T})$ the set of edges of $\mathcal{T}$. To discretize advection-diffusion problems on these triangular meshes, we suggest a combination of the approach of Kurganov and Petrova in [37] for the hyperbolic part and the discretization of parabolic fluxes as in the approach of Eymard, Gallouët, and Herbin in [13]. The use of equilateral triangles ensures the consistent discretization of the parabolic fluxes by evaluation in the centers of gravity.

This method-of-lines approach is completed by the forward Euler scheme in time. To this end let $t^0 := 0 < t^1 < \cdots < t^N := T$ for $N \in \mathbb{N}$ be a partition of $(0,T)$ with time step $\Delta t^n = t^{n+1} - t^n$ for $n \in \{0, \dots, N-1\}$.

All in all, one gets a scheme, which is first-order accurate in space and time.

DEFINITION 5.1 (finite volume method on a domain ω). *For $n \in \{0, \dots, N-1\}$ and each triangle $\mathcal{T}$ of the triangulation $\mathcal{T}_{\omega,\Delta x}$, the approximate cell average $u_{\mathcal{T}}^{n+1}$ at time t^{n+1} is computed by*

$$u_{\mathcal{T}}^{n+1} = u_{\mathcal{T}}^{n} - \frac{\Delta t^n \Delta x}{|\mathcal{T}|} \sum_{\sigma \in \mathcal{S}(\mathcal{T})} F_\sigma^n. \tag{5.1}$$

If σ is the edge of another triangle $\mathcal{T}' \in \mathcal{T}_{\omega,\Delta x}$ the numerical flux F_σ^n is given by

$$F_\sigma^n := -\frac{P(u_{\mathcal{T}'}^n) - P(u_{\mathcal{T}}^n)}{\Delta x/\sqrt{3}} + \left(\frac{a_\sigma^{in}\mathbf{f}(u_{\mathcal{T}'}^n) + a_\sigma^{out}\mathbf{f}(u_{\mathcal{T}}^n)}{a_\sigma^{in} + a_\sigma^{out}} \right) \cdot \mathbf{n}_{\mathcal{T}} - \frac{a_\sigma^{in} a_\sigma^{out}}{a_\sigma^{in} + a_\sigma^{out}} \left(u_{\mathcal{T}'}^n - u_{\mathcal{T}}^n \right). \tag{5.2}$$

For $\sigma \in \partial\omega \cap \partial\Omega$ the flux F_σ^n is determined from the boundary conditions (depending on specific settings in section 6), whereas for $\sigma \in \partial\omega \cap \Gamma$ the flux F_σ^n is defined from the discrete transmission conditions (see (5.7) below). The initial approximation $u_{\mathcal{T}}^0$ is set as approximation of the cell average. For our first-order method, we use simply $u_{\mathcal{T}}^0 = u_0(\mathbf{x}_{\mathcal{T}})$, with $\mathbf{x}_{\mathcal{T}}$ denoting the barycenter of $\mathcal{T}$.

As before the function $P = P(u)$ in (5.2) is a primitive of $p(u)$. The numbers $a_\sigma^{in}, a_\sigma^{out} \geq 0$ are estimated local inward and outward directional wave speeds at an edge σ of $\mathcal{T}$, which has the outer normal $\mathbf{n}_{\mathcal{T}}$. These choices imply that the numerical algorithm from Definition 5.1 can be applied for any directional flux $\mathbf{f} \cdot \mathbf{n}_{\mathcal{T}}$ regardless of its derivative sign; see [37]. However, it recovers the upwind flux depending on the sign.

Due to the time-explicit approach, the size of the time-step Δt^n is limited by the Courant–Friedrichs–Lewy condition and the Péclet condition

$$\max\left\{ \left(\max_u |f_1'(u)| + \max_u |f_2'(u)| \right) \frac{\Delta t^n}{\Delta x},\ \max_u p(u) \frac{2\Delta t^n}{\Delta x^2} \right\} \leq C_{\max}. \tag{5.3}$$

The constant $C_{\max} \leq 1$ depends on the mesh topology.

Having computed the cell-average values $u_{\mathcal{T}}^n$ on the mono-domain, we define the discrete solution $u_{\Omega,\Delta x} \in L^2(\Omega \times (0,T))$ as a piecewise constant function by

$$u_{\Omega,\Delta x}(\mathbf{x}, t) = u_{\mathcal{T}}^n, \qquad \mathbf{x} \in \mathcal{T} \subset \mathcal{T}_{\Omega,\Delta x},\ t \in [t^n, t^{n+1}). \tag{5.4}$$

The finite-volume computations on the sub-domains Ω_1, Ω_2 have to be redone in each iteration within the SWR algorithm. We denote for $k \in \mathbb{N}$ the corresponding cell-average values therefore by $u_{\mathcal{T}}^{k,n}$, the numerical fluxes by $F_\sigma^{k,n}$, and the discrete solution by $u_{\omega,\Delta x}^k \in L^2(\omega \times (0,T))$ with ω being one of the sub-domains Ω_1, Ω_2. It is again computed from the cell averages, i.e.,

$$u_{\omega,\Delta x}^k(\mathbf{x}, t) = u_{\mathcal{T}}^{k,n}, \qquad \mathbf{x} \in \mathcal{T} \subset \mathcal{T}_{\omega,\Delta x},\ t \in [t^n, t^{n+1}). \tag{5.5}$$

5.2. Discretization of the transmission condition. To complete the discrete SWR algorithm we need besides initial iterates a discrete version of the transmission condition (2.9) that provides the numerical flux in Definition 5.1 across some edge on Γ.

We assume that the meshes for $\Omega, \Omega_1, \Omega_2$ are designed such that the interface $\Gamma = \{0\} \times (-1, 1)$ between the sub-domains coincides with the edges of the triangles.

To compute a numerical flux on Ω_1 (the case for the right sub-domain is completely analogous) consider a pair $(\mathcal{T}, \mathcal{T}') \subset \Omega_1 \times \Omega_2$ such that these two triangles share an edge σ which lies on Γ. Following [24], we search a ghost value $u_{\sigma,1}^{k,n}$ as approximation of the discrete solution in the triangle $\mathcal{T}'$ on the other side of the edge σ. This value is used to compute the flux $F_\sigma^{k,n} = F_{\sigma,1}^{k,n}$.

Due to the transmission condition (2.9), in the kth SWR iteration and at discrete time t^n, the discrete normal flux $F_{\sigma,1}^{k,n}$ associated to the triangle $\mathcal{T}$ on this edge is then given by (5.2) as

$$F_{\sigma,1}^{k,n} := -\frac{P(u_{\sigma,1}^{k,n}) - P(u_{\mathcal{T}}^{k,n})}{\Delta x/\sqrt{3}} + \left(\frac{a_\sigma^{in}\mathbf{f}(u_{\sigma,1}^{k,n}) + a_\sigma^{out}\mathbf{f}(u_{\mathcal{T}}^{k,n})}{a_\sigma^{in} + a_\sigma^{out}}\right)\cdot \mathbf{n}_{\mathcal{T}} - \frac{a_\sigma^{in}a_\sigma^{out}}{a_\sigma^{in} + a_\sigma^{out}}\left(u_{\sigma,1}^{k,n} - u_{\mathcal{T}}^{k,n}\right), \tag{5.6}$$

such that $u_{\sigma,1}^{k,n}$ satisfies (see (2.9))

$$F_{\sigma,1}^{k,n} = \lambda\big(\beta_1 u_{\mathcal{T}}^{k,n} + (1-\beta_1)u_{\sigma,1}^{k,n}\big) - \mathfrak{B}_{\sigma,1}^{k,n}. \tag{5.7}$$

Analogously, for Ω_2, we have to compute $F_{\sigma,2}^{k,n}$, which leads us to determine $u_{\sigma,2}^{k,n}$ from

$$F_{\sigma,2}^{k,n} = \lambda\big(\beta_2 u_{\mathcal{T}'}^{k,n} + (1-\beta_2)u_{\sigma,2}^{k,n}\big) - \mathfrak{B}_{\sigma,2}^{k,n}. \tag{5.8}$$

The weighting parameters β_1, β_2 in (5.7), (5.8) are taken from the interval $[0,1]$. They allow us to interpolate between the cell average and the ghost value at the interface, and they have no counterpart at the continuous level. In [24] we analyzed a simple linear model problem and showed that introducing the weighting parameters can be used to construct discrete SWR algorithms that are convergent for $\Delta x \to 0$ and $k \to \infty$, consistent for fixed Δx and $k \to \infty$, and asymptotic preserving for vanishing viscosity (see section 6.1 for precise definitions). We cannot transfer the proofs to the nonlinear case here, but we will show in section 6 that the preferred choice from [24] remains to be effective in our case.

We will use two choices for β_1, β_2. The first one accounts for the local transport direction at the edge σ. It is considered to be a novel contribution for the treatment of advection-diffusion equations. Motivated by the analysis for a linear one-dimensional model problem in [24], it is defined by

(A) $$\beta_1 = \begin{cases} \frac{1}{2}, & \mathbf{f}'(u_{\mathcal{T}}^{k,n})\cdot\mathbf{n}_{\mathcal{T}} \geq 0, \\ 0 & \text{otherwise,} \end{cases} \quad \text{and} \quad \beta_2 = \begin{cases} \frac{1}{2}, & \mathbf{f}'(u_{\mathcal{T}'}^{k,n})\cdot\mathbf{n}_{\mathcal{T}'} \geq 0, \\ 0 & \text{otherwise.} \end{cases}$$

Note that this first choice (A) realizes a switch between a centered approximation and a pure upwind one. In section 6.3.2 we will show that (A) behaves much better in the hyperbolic limit regime than the second choice, which is a pure centered approximation, typically used for diffusion equations (realizing a second-order discretization in space). It is given by

(B) $$\beta_1 = \beta_2 = \frac{1}{2}.$$

It remains to define $\mathfrak{B}_{\sigma,1}^{k,n}$ and $\mathfrak{B}_{\sigma,2}^{k,n}$ in (5.7) and (5.8). The value $\mathfrak{B}_{\sigma,1}^{k,n}$ is computed based on (2.9) from the previous SWR iteration using (5.6) and (5.7) with $u_{\mathcal{T}'}^{k-1,n}$

and $u_{\sigma,2}^{k-1,n}$ replacing $u_{\sigma,1}^{k,n}$ and $u_{\mathcal{T}}^{k,n}$. The analogous procedure provides $\mathfrak{B}_{\sigma,2}^{k,n}$. An alternative definition not used here exploits (2.12) leading for Ω_1 to $\mathfrak{B}_{\sigma,1}^{k,n} := \lambda((1+\beta_1-\beta_2)u_{\sigma,2}^{k-1,n} + (1-\beta_1+\beta_2)u_{\mathcal{T}}^{k-1,n}) - \mathfrak{B}_{\sigma,2}^{k-1,n}$. Finally, the initial guesses g_1 in all considered cases are chosen as discrete approximations of $\mathfrak{B}_1(u_0)$ using (2.9).

Even though the time stepping in the scheme from Definition 5.1 is explicit, the unknowns $u_{\sigma,i}^{k,n}$ for $i \in \{1,2\}$ at the interface have to be determined from the generally nonlinear equations (5.6) and (5.7). We use a damped Newton method and emphasize that only a local Newton iteration for each triangle at the interface has to be performed.

6. Numerical results. First, we consider a simple problem with known closed-form solution to study both the convergence properties of the discretization and the iterative solver. We then study the performance of the solver on the two-phase equation for the saturated flow of two immiscible and incompressible fluids. In particular, we are interested in the behavior of the SWR algorithm for advection-dominated flow and in the role of the transmission parameter λ and the weighting parameters β_1, β_2 in the transmission conditions.

Before we start with some preliminaries on error measurement and associated notations let us note that various non-overlapping domain decomposition approaches have been developed in the context of two-phase flow. Ahmed et al. have studied a posteriori error estimates and stopping criteria based on space-time domain decomposition for two-phase flow between different rock types in [1, 2]. Seus et al. proposed robust linear domain decomposition methods of the time-discrete equations for partially saturated flow as well as for two-phase flow in porous media in [47, 48]. This was extended in [42] by Lunowa, Pop, and Koren for two-phase flow in porous media involving dynamic capillarity and hysteresis. For domain decomposition strategies used as preconditioners for solving multi-phase flow problems we refer the reader to [49].

6.1. Error functionals and notations. We introduce some notations for measuring different kinds of errors. Precisely, we use two functionals: for studying the convergence of the iterative algorithm, we fix the mesh parameter Δx and use the mono-domain finite volume solution $u_{\Omega,\Delta x}$ from (5.4). We define the iteration space-time L^2-*error* $\mathcal{E}_{\Delta x}^k$ given by

$$\mathcal{E}_{\Delta x}^k := \sqrt{\sum_{i=1,2} \left\| u_{\Omega_i,\Delta x}^k - u_{\Omega,\Delta x}\big|_{\Omega_i\times(0,T)} \right\|_{L^2(\Omega_i\times(0,T))}^2}. \tag{6.1}$$

It controls the distance between the discrete SWR iterates on the sub-domains Ω_1, Ω_2 and the discrete mono-domain solution on Ω. The SWR algorithm is *consistent* with respect to iterations if $\mathcal{E}_{\Delta x}^k \to 0$ holds for $k \to \infty$. The SWR algorithm is *asymptotic-preserving* in the limit of vanishing viscosity if it converges then in a finite number of iterations, i.e., there holds $\mathcal{E}_{\Delta x}^k = 0$ for all $k > k_0 \in \mathbb{N}$ when $p \equiv 0$. This means that the limit SWR algorithm behaves as expected of domain decomposition methods for hyperbolic PDEs; for details on this issue see, e.g., [24].

If the exact solution u is available we also consider the difference between the SWR iterates $u_{\Omega_i,\Delta x}^k$ (see (5.5)) and the exact solution u leading to the combined iteration and discretization space-time L^2-*error* $\tilde{\mathcal{E}}_{\Delta x}^k$ defined by

$$\tilde{\mathcal{E}}_{\Delta x}^k := \sqrt{\sum_{i=1,2} \left\| u_{\Omega_i,\Delta x}^k - u\big|_{\Omega_i\times(0,T)} \right\|_{L^2(\Omega_i\times(0,T))}^2}. \tag{6.2}$$

If $\tilde{\mathcal{E}}_{\Delta x}^k \to 0$ for $\Delta x \to 0$, $k \to \infty$ the SWR algorithm *converges* to u.

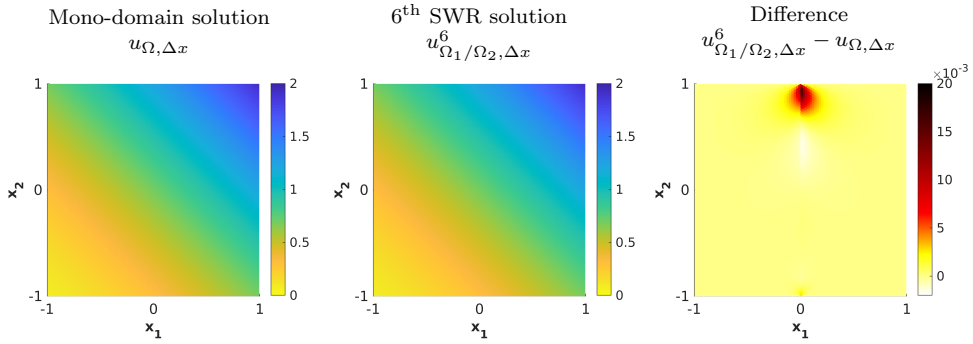

FIG. 6.1. *The numerical mono-domain solution* (left) *and the SWR solution at the* 6*th iteration* (middle) *are hardly distinguishable from each other for the smooth example at* $t = 2$ *using* $\Delta x = 0.025$ *and* $\lambda = 1.5$. *In fact, the errors are concentrated almost entirely at the interface* (right).

In addition to the behavior of $\mathcal{E}^k_{\Delta x}$ and $\tilde{\mathcal{E}}^k_{\Delta x}$ for $\Delta x \to 0$ and $k \to \infty$ we will also investigate how the limit behavior of the SWR algorithm depends on the transmission parameter λ.

6.2. A problem with known solution. The function

$$u(\mathbf{x}, t) = \frac{(3 + x_1 + x_2)^2}{25 - 6t}$$

solves the nonlinear advection-diffusion equation

$$\partial_t u + \operatorname{div}(\mathbf{v}u^2) - \operatorname{div}(u\nabla u) = 0 \qquad \text{in} \quad \Omega \times (0,T) := (-1,1)^2 \times (0,2), \tag{6.3}$$

where the velocity $\mathbf{v} = \mathbf{v}(\mathbf{x})$ is given by $\mathbf{v}(\mathbf{x}) = \frac{1}{3+x_1+x_2}(1,1)^T$. The problem is completed by Dirichlet boundary conditions and an initial condition given by evaluating u on $\partial\Omega$ and at $t = 0$.

For the numerical solution, we choose the temporal step-size $\Delta t = (\Delta x)^2/25$ (which suffices in this case to satisfy (5.3)) and the SWR transmission parameter $\lambda = 1.5$.

The plots in Figure 6.1 show the results of the finite volume method on the mono-domain Ω and of the SWR algorithm with parameter choice (A), where we have chosen the sixth iteration with $\Delta x = 0.025$ at time $t = 2$. Clearly, the error is concentrated at the interface Γ, especially where the flux across the interface is large.

In Figure 6.2 we see on the left that the iteration L^2-error $\mathcal{E}^k_{\Delta x}$ from (6.1) decreases monotonically for versions (A) and (B), suggesting that the SWR algorithm is consistent for both choices of the weighting parameters. Note that our convergence analysis does not predict a monotonic behavior. The fact that the convergence does not seem to depend on the spatial step-size is because we start the iteration by extending the initial condition constant in time, and the solution and thus the iterations do not really have any high frequency content. Using a random initial guess would lead to different behavior; see [21] for linear problems with constant coefficients, where mesh dependence is observed, and [17, Sec. 5.1] for a detailed explanation.

Since we know the exact solution in this case, we can also compute the combined discretization and iteration L^2-error $\tilde{\mathcal{E}}^k_{\Delta x}$ from (6.2). As shown in Figure 6.2 on the right, we observe that $\tilde{\mathcal{E}}^k_{\Delta x} \to 0$ for $\Delta x \to 0$ and $k \to \infty$ supporting the convergence statement of Theorem 4.1. We observe for a fixed mesh parameter again a monotone

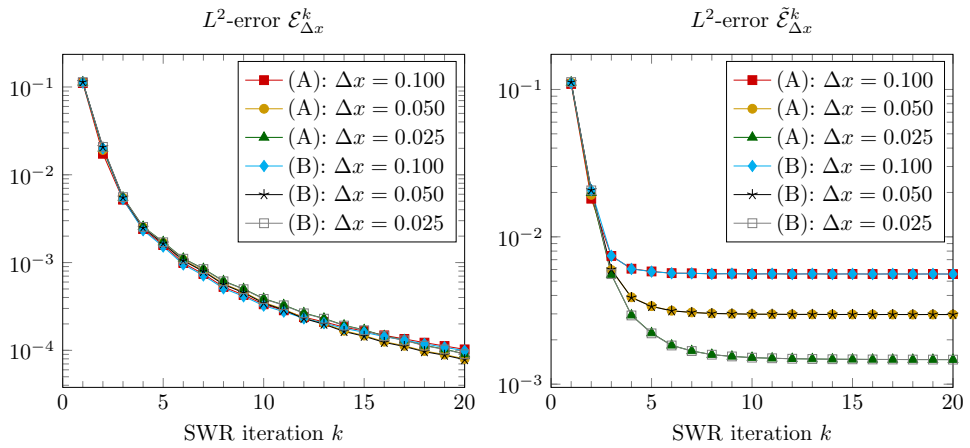

FIG. 6.2. *Error decay for the different spatial resolutions in the example with known solution using* $\lambda = 1.5$ *and both choices* (A) *and* (B). Left: *the iteration* L^2*-error* $\mathcal{E}^k_{\Delta x}$ *decreases monotonically.* Right: *the combined iteration and discretization* L^2*-error* $\tilde{\mathcal{E}}^k_{\Delta x}$ *also decreases monotonically until the discretization error level is reached after a few iterations.*

decay of $\tilde{\mathcal{E}}^k_{\Delta x}$ over the SWR iterations. After about 3–5 iterations, the discretization error clearly dominates, and we observe stagnation of the combined discretization and iteration error. The discretization error is approximately reduced by a factor of two when halving the spatial step-size Δx, as expected for a first-order scheme. Again versions (A) and (B) do not differ substantially.

Let us fix the spatial step-size to $\Delta x = 0.05$ and use the choice (A) only. To study the effect of the transmission parameter, we apply the SWR iteration for different choices of the transmission parameter λ. The impact on the convergence rate is clearly visible from the results shown in Figure 6.3. On the left, we see that an optimal choice of λ exists which leads to fastest convergence of the SWR iteration for the specific frequency content in the solution. We also see that after a certain number of iterations the slopes of the convergence curves become similar, and in that regime typically very high or very low frequency error components dominate. On the right we see that the truncation error accuracy is however reached much earlier, so a good choice is indeed $\lambda = 1.5$ for this problem.

6.3. Simplified two-phase flow with capillary pressure. We consider a nonlinear advection-diffusion equation that is used to model the incompressible flow of two immiscible fluids in a porous medium, such as the displacement of oil by water in a reservoir. This model can be derived from the mass conservation equations of two-phase flow and a generalized Darcy relation [36]. Neglecting gravitational effects, we obtain for a given total velocity $\mathbf{v} : \Omega \to \mathbb{R}^d$ the equation

$$\phi \partial_t u + \operatorname{div}\left(\mathbf{v} f_{BL}(u)\right) + \operatorname{div}\left(\kappa(u) K \nabla p_c(u)\right) = 0 \qquad \text{in} \quad \Omega \times (0,T). \tag{6.4}$$

The saturation $u = u(\mathbf{x}, t) \in [0,1]$ is the unknown, whereas the porosity $\phi \in (0,1]$, the fractional flux function $f_{BL} : [0,1] \to \mathbb{R}$, the total mobility $\kappa : [0,1] \to (0,\infty)$, the homogeneous intrinsic permeability $K \in \mathbb{R}^{d\times d}$, and the capillary pressure $p_c : [0,1] \to \mathbb{R}$ are given functions. For our numerical studies, we simply choose the domain $\Omega := (-1,1)^2$, the final time $T = 1$, as well as a constant porosity $\phi = 1$ and a constant flow velocity $\mathbf{v} = (v_1, v_2)^T \in \mathbb{R}^2$. The constant intrinsic permeability K

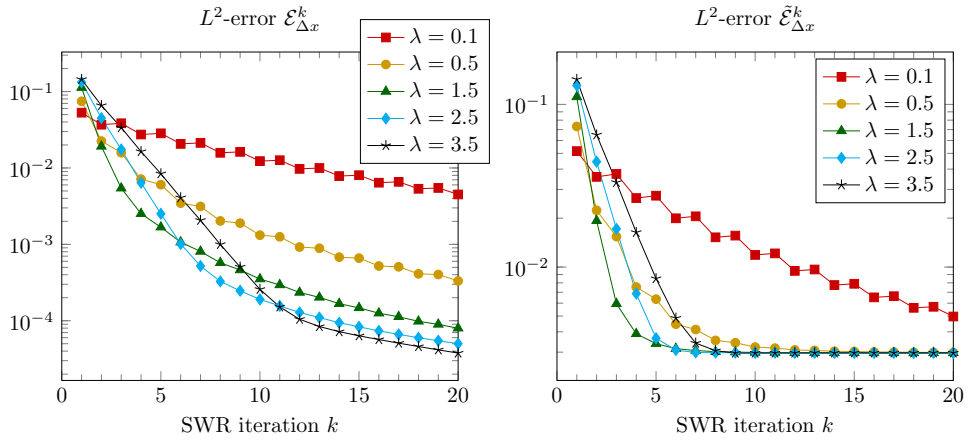

FIG. 6.3. *Error decay over the number of SWR iterations for different transmission parameters λ in the example with exact solution using $\Delta x = 0.05$ and the choice* (A). *Left: Iteration L^2-error$\mathcal{E}^k_{\Delta x}$. Right: Combined discretization and iteration L^2-error $\tilde{\mathcal{E}}^k_{\Delta x}$.*

is set to be the identity matrix, and a standard parametrization of the fractional flux function is

$$f_{BL}(u) = \frac{u^2}{u^2 + (1-u)^2}.$$

For $\kappa \equiv 0$, (6.4) becomes the so-called Buckley–Leverett equation, which is a purely hyperbolic conservation law exhibiting weak discontinuous solutions.

6.3.1. Diffusion-dominated regimes. We consider a simplified setting with linear capillary pressure, $p_c(u) = 1 - u$. The problem is completed with the initial condition $u_0 \equiv 0$ and the Dirichlet boundary condition given for $\mathbf{x} \in \partial\Omega$ and $t \in [0, 1]$ by

$$u(\mathbf{x}, t) = \begin{cases} 1 - x_2^2 & \text{if } x_1 = -1, \\ 0 & \text{if } x_1 = 1 \text{ or } x_2 = \pm 1. \end{cases}$$

Thus, the solution of (6.4) will display a right-moving infiltration front as long as the velocity components satisfy $v_1 > v_2 \equiv 0$. In fact, this will be our choice in all subsequent experiments. As an internal layer the front will scale according to the size of the (assumed to be) constant mobility parameter κ. For the sake of illustration we show in Figure 6.4 the results of a mono-domain computation and the sixth iteration of the SWR algorithm at the final time $t = 1$. Clearly, the difference of these discrete solutions prevails at the interface Γ and the infiltration front. Since the flow direction is from left to right, the errors occur almost entirely in the second sub-domain.

Turning to quantitative tests of the SWR algorithm, we consider in this section examples which can include advection but are still diffusion-dominated. Since explicit solutions for (6.4) are not available, we study the iteration L^2-error $\mathcal{E}^k_{\Delta x}$ only. In the first example, condition (5.3) is satisfied by choosing the time step-size $\Delta t^n = \Delta x^2/20$. The SWR transmission parameter is fixed to be $\lambda = 2$.

In Figure 6.5 we show the results for a fixed mobility $\kappa = 1$ varying the velocity v_1 in the x_1-direction for different mesh resolutions. As a purely diffusive reference case we consider $v_1 = 0$ such that (6.4) becomes the heat equation (see also the results

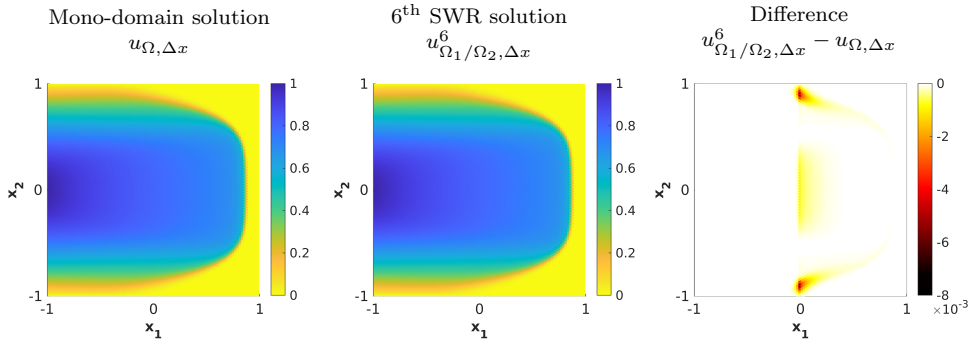

FIG. 6.4. *Discrete mono-domain solution* (left) *and SWR solutions at the 6th iteration* (middle) *for the simplified two-phase equation for* $\kappa = 10^{-2}$, $\mathbf{v} = (1.5, 0)^T$ *at time* $t = 1$ *using* $\Delta x = 0.025$, $\lambda = 2$, *and weighting parameters from* (A). *The errors are concentrated almost entirely at the interface* Γ *and along the infiltration front* (right).

in section 6.3.2 for the opposite limit case: the Buckley–Leverett equation). For all mesh parameters we observe that the iteration error $\mathcal{E}^k_{\Delta x}$ decreases monotonically in k. Moreover, the difference between the weighting parameter choices (A) and (B) is negligible.

Next, we study again the impact of the transmission parameter. We set $\Delta x = 0.05$ or $\Delta x = 0.025$ and $\Delta t^n = \Delta x/20$, and we apply the SWR iteration with different choices of the transmission parameter λ, with $\mathbf{v} = (1.5, 0)^T$ and $\kappa = 10^{-2}$, i.e., a more advection-dominated regime which triggers a step-like behavior for the evolution of $\mathcal{E}^k_{\Delta x}$. The effect of the transmission parameter on the convergence rate is clearly visible from the results shown in Figure 6.6, the best choice here being around $\lambda = 1.5$. We also observe that the weighting choice (B) is not equivalent in the present discretization when advection becomes dominant (see, e.g., (B): $\lambda = 2$ in Figure 6.6) because it remains a Robin transmission condition, while choice (A) effectively leads to a Dirichlet update in the hyperbolic limit $\kappa \to 0$; cf. [24].

Furthermore, we study the numerical scheme for a decomposition into multiple sub-domains; see Figure 6.7. As in the case of two sub-domains, the discrete difference, and hence the iteration L^2-error $\mathcal{E}^k_{\Delta x}$, is reduced in a step-like manner in the first few iterations and shows linear convergence, but at a slightly lower rate compared to the case of only two sub-domains.

6.3.2. From advection-dominated regimes to the hyperbolic limit. We investigate the SWR algorithm for the same infiltration setting as in section 6.3.1 but fixing $\mathbf{v} = (1.5, 0)^T$ and focusing on decreasing values of the total mobility κ. If the mesh parameter Δx is kept constant for advection-dominated regimes, one enters under-resolved situations. Note that the finite-volume scheme from Definition 5.1 remains even then stable due to the upwind flux choice [37]. However, it is not able to resolve (internal and boundary) layers scaling like $\mathcal{O}(\kappa)$. In the limit $\kappa \to 0$, (6.4) becomes a purely hyperbolic evolution law with discontinuous weak solutions. Notably, the sub-domain problems of the SWR algorithm given by Definition 2.3 are not well defined in the hyperbolic limit; i.e., the Robin boundary condition (2.8) and (2.9) involve Neumann traces that might not exist. Nevertheless, the discrete formulation by Definition 5.1 together with (5.6) and (5.7) can still be executed.

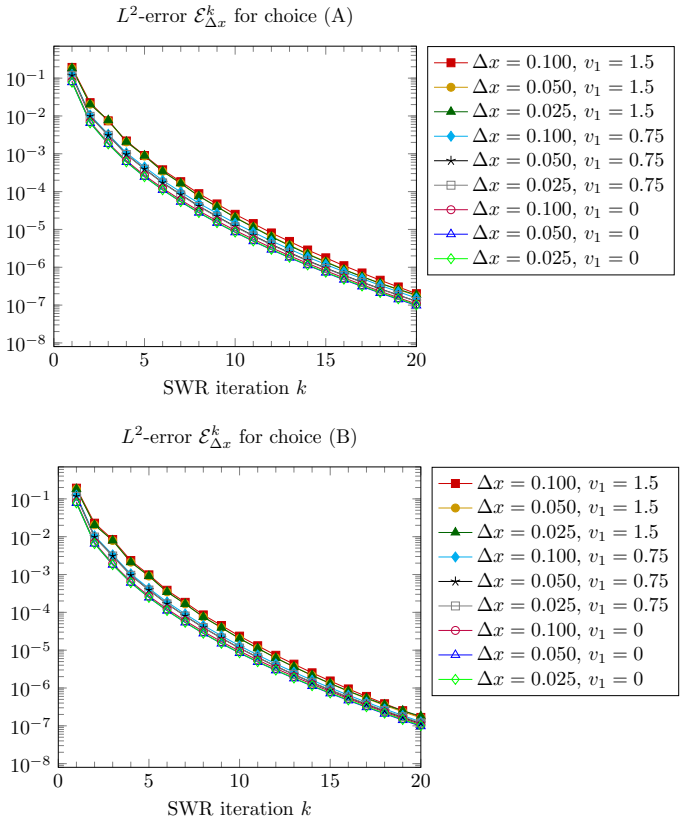

FIG. 6.5. *The iteration L^2-error versus the number of SWR iterations for different spatial resolutions and different velocities $\mathbf{v} = (v_1, 0)^T$. The mobility is always $\kappa = 1$.*

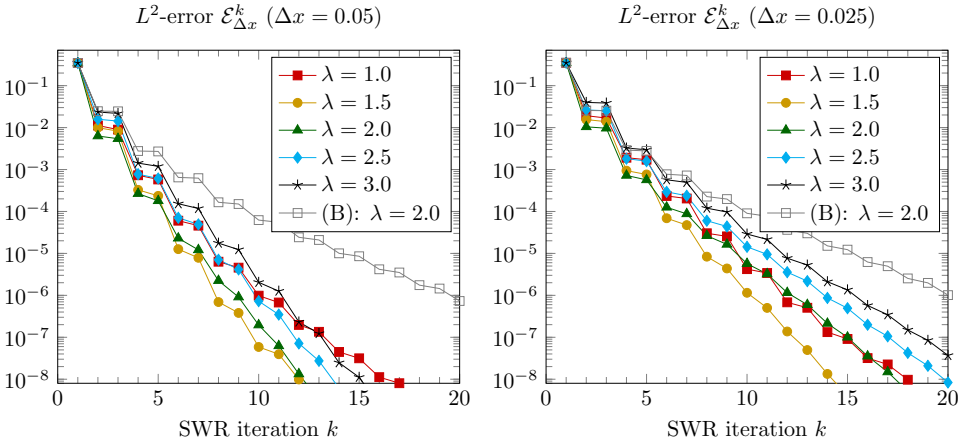

FIG. 6.6. *The decay of the L^2-error over the number of SWR iterations varies for different transmission parameters λ for the simplified two-phase equation with $\Delta x = 0.05$ and $\Delta x = 0.025$ using the choice* (A). *The optimum $\lambda \approx 1.5$ seems to be independent of the step-size for this initial guess.*

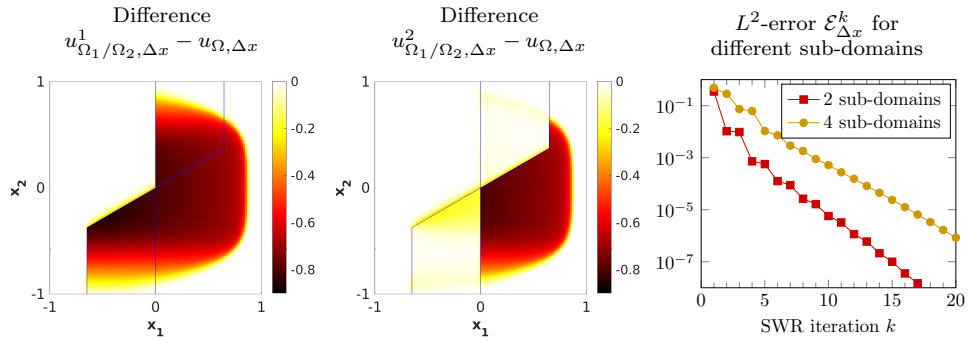

FIG. 6.7. *The discrete difference at the* 1*st* (left) *and* 2*nd* (middle) *iterations for four sub-domains in the case of the simplified two-phase equation* ($\kappa = 10^{-2}$, $\mathbf{v} = (1.5, 0)^T$, $t = 1$, $\Delta x = 0.025$, $\lambda = 2$, *weighting* (A)*). The interfaces are shown in blue. The iteration* L^2*-error decays linearly, but slightly slower compared to the case of only two sub-domains* (right) *(Color available online).*

Remark 6.1 (SWR algorithm for the hyperbolic limit, choice of λ, β_1, and β_2). For the case $\kappa = 0$ the SWR algorithm using Dirichlet transmission conditions gives the mono-domain solution on Ω in finitely many steps, for the unidirectional flux in (6.4) in fact in two steps only. Using Robin transmission conditions as in (5.7) requires further conditions for this property to hold [24]: in the linear case, the algorithm is asymptotic-preserving iff the parameters β_1, β_2 are chosen to satisfy $\kappa/\beta_1(\kappa) = o(1)$ and $\beta_2(\kappa) = \mathcal{O}(\kappa)$ as $\kappa \to 0$. Since this condition is independent of λ, we expect similar behavior here and illustrate this below. Note that choice (A) satisfies the conditions, but (B) does not.

We consider the advection-dominated regime for $\kappa \in (0, 10^{-2}]$ and set $\Delta x = 0.025$ and $\Delta t^n = \Delta x/20$. All other settings are as in section 6.3.1. In Figure 6.8 we show the L^2-errors $\mathcal{E}^k_{\Delta x}$ for weighting parameters from (A). As in section 6.3.1 we observe linear convergence, which gets faster as κ becomes smaller, until we get two-step convergence for $\kappa = 0$ ($\mathcal{E}^2_{\Delta x} < 10^{-12}$) independently of the value of the transmission parameter. This is also in agreement with the analysis for linear problems; see Remark 6.1. We note in passing that using the alternative determination of $\mathfrak{B}^{k,n}_{\sigma,1/2}$ using (2.12) shows also decaying behavior but requires four iterations in the limit.

On the right in Figure 6.8 we show the results for the transmission condition update (B), which clearly is not equivalent to (A) in the present discretization; see the discussion in the previous subsection: the choice (B) is not asymptotic preserving.

6.4. Two-phase flow with strongly nonlinear capillary pressure: Brooks–Corey parametrization. As a concluding example we consider the two-phase equation (6.4), together with the Brooks–Corey model [36],

$$\kappa(u) = \frac{u^2(1-u)^2}{u^2 + (1-u)^2}, \qquad p_c(u) = p_d u^{-\frac{1}{\lambda_{BC}}}.$$

Here $p_d > 0$ is the so-called entry pressure, i.e., the minimal pressure necessary for the non-wetting phase to displace the wetting phase, and $\lambda_{BC} > 0$ describes the uniformity of the porous medium. We choose the parameters $p_d = 1$ and $\lambda_{BC} = 3$ and the initial condition $u_0 = 0.1$ together with homogeneous Neumann boundary

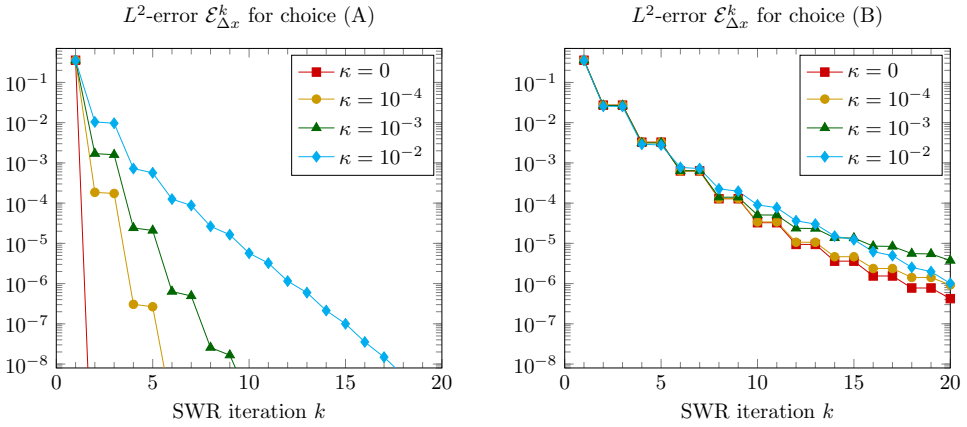

FIG. 6.8. *The L^2-errors $\mathcal{E}^k_{\Delta x}$ for $\lambda = 2$ and step-size $\Delta x = 0.025$. Left: For the choice* (A)*, the rate of decay of $\mathcal{E}^k_{\Delta x}$ over the number of SWR iterations depends on total mobility κ strongly improving when κ decreases. Right: For the choice* (B)*, the rate of decay does not improve to finite-step convergence in the hyperbolic limit when $\kappa \to 0$.*

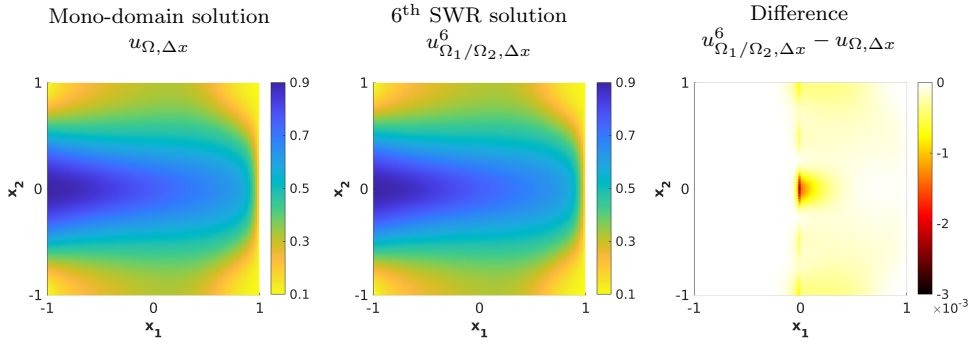

FIG. 6.9. *The numerical mono-domain solution* (left) *and the SWR solution at the 6th iteration* (middle) *are hardly distinguishable from each other for the two-phase equation with Brooks–Corey parametrization at $t = 1$ using $\Delta x = 0.025$. Differences can be observed mostly at the interface Γ but less for the wave-front position* (right).

conditions at $x_2 = \pm 1$, and Dirichlet boundary conditions at $x_1 = \pm 1$ given by

$$u(\mathbf{x}, t) = \begin{cases} 0.1 + 0.8(1 - x_2^2)^2 & \text{if } x_1 = -1, \\ 0.1 & \text{if } x_1 = 1. \end{cases}$$

For the numerical computations of this completely nonlinear infiltration problem, we select the temporal step-size $\Delta t = (\Delta x)^2/4$ and the SWR transmission parameter $\lambda = 2$. According to the results from section 6.3.2 we use choice (A) only. The plots in Figure 6.9 show the results with and without the SWR algorithm for the sixth SWR iteration and $\Delta x = 0.025$ at time $t = 1$. Also for this strongly nonlinear problem, the error is concentrated at the interface Γ and in Ω_2, since the flow direction is from left to right. The error decreases monotonically over the SWR iterations, as shown in Figure 6.10.

7. Conclusion. We designed and analyzed a new non-overlapping Schwarz waveform-relaxation algorithm for nonlinear advection-diffusion equations using non-

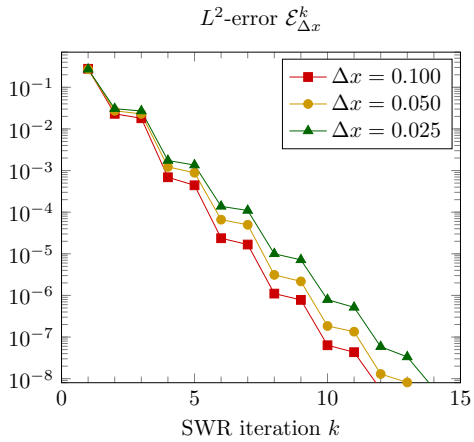

FIG. 6.10. *The L^2-error $\mathcal{E}^k_{\Delta x}$ decreases monotonically over the number of SWR iterations for the different spatial resolutions for the two-phase equation with Brooks–Corey parametrization with $\lambda = 2.5$.*

linear Robin transmission conditions. We proved existence of a unique sequence of weak solutions that converges under the assumption of bounded gradients, extending the area of application of Schwarz waveform-relaxation to a whole new class of nonlinear problems. We also presented a fully discrete finite volume scheme which is asymptotic preserving for the Robin transmission conditions and hence robust in the hyperbolic limit, leading to two-step convergence of the iterative solver. We tested our new solver on several examples ranging from validation models to strongly nonlinear porous media flow problems. We observed linear convergence towards the discrete solution, and robust two-step convergence in the hyperbolic limit. We also conducted preliminary numerical tests for the impact of the transmission parameter λ on the convergence rate, for which we do not yet have a theoretical basis.

REFERENCES

[1] E. AHMED, S. A. HASSAN, C. JAPHET, M. KERN, AND M. VOHRALÍK, *A posteriori error estimates and stopping criteria for space-time domain decomposition for two-phase flow between different rock types*, SMAI J. Comput. Math., 5 (2019), pp. 195–227.

[2] E. AHMED, C. JAPHET, AND M. KERN, *Space-time domain decomposition for two-phase flow between different rock types*, Comput. Methods Appl. Mech. Engrg., 371 (2020), 113294.

[3] H. W. ALT AND S. LUCKHAUS, *Quasilinear elliptic-parabolic differential equations*, Math. Z., 183 (1983), pp. 311–341.

[4] H. AMANN, *Maximal regularity of parabolic transmission problems*, J. Evol. Equ., 21 (2021), pp. 3375–3420.

[5] D. BENNEQUIN, M. J. GANDER, L. GOUARIN, AND L. HALPERN, *Optimized Schwarz waveform relaxation for advection reaction diffusion equations in two dimensions*, Numer. Math., 134 (2016), pp. 513–567.

[6] D. BENNEQUIN, M. J. GANDER, AND L. HALPERN, *A homographic best approximation problem with application to optimized Schwarz waveform relaxation*, Math. Comput., 78 (2009), pp. 185–223.

[7] M. BJØRHUS, *On Domain Decomposition, Subdomain Iteration and Waveform Relaxation*, Ph.D. thesis, University of Trondheim, Trondheim, Norway, 1995.

[8] C.-H. BRUNEAU AND P. FABRIE, *New efficient boundary conditions for incompressible Navier-Stokes equations: A well-posedness result*, RAIRO Modél Math. Anal. Numér., 30 (1996), pp. 815–840.

[9] F. CAETANO, M. J. GANDER, L. HALPERN, AND J. SZEFTEL, *Schwarz waveform relaxation algorithms for semilinear reaction-diffusion equations*, Netw. Heterog. Media, 5 (2010), pp. 487–505.

[10] O. Ciobanu, L. Halpern, X. Juvigny, and J. Ryan, *Overlapping domain decomposition applied to the Navier-Stokes equations*, in Domain Decomposition Methods in Science and Engineering XXII, Lect. Notes Comput. Sci. Eng. 104, Springer, Cham, 2016, pp. 461–470.
[11] V. Dolean, P. Jolivet, and F. Nataf, *An Introduction to Domain Decomposition Methods: Algorithms, Theory, and Parallel Implementation*, SIAM, Philadelphia, 2015.
[12] L. C. Evans, *Partial Differential Equations*, 2nd ed., Grad. Stud. Math., AMS, Providence, RI, 2010.
[13] R. Eymard, T. Gallouët, and R. Herbin, *Finite volume methods*, in Handbook of Numerical Analysis, vol. 7, P. Ciarlet and J. Lions, eds., North-Holland, Amsterdam, 2000, pp. 713–1020.
[14] M. J. Gander, *Overlapping Schwarz for linear and nonlinear parabolic problems*, in Proceedings of the 9th International Conference on Domain Decomposition, ddm.org, 1996, pp. 97–104.
[15] M. J. Gander, *A waveform relaxation algorithm with overlapping splitting for reaction diffusion equations*, Numer. Linear Algebra Appl., 6 (1998), pp. 125–145.
[16] M. J. Gander, *Optimized Schwarz methods*, SIAM J. Numer. Anal., 44 (2006), pp. 699–731, https://doi.org/10.1137/S0036142903425409.
[17] M. J. Gander, *Schwarz methods over the course of time*, Electron. Trans. Numer. Anal., 31 (2008), pp. 228–255.
[18] M. J. Gander, *50 years of time parallel time integration*, in Multiple Shooting and Time Domain Decomposition Methods, Springer, New York, 2015, pp. 69–113.
[19] M. J. Gander, L. Gouarin, and L. Halpern, *Optimized Schwarz waveform relaxation methods: A large scale numerical study*, in Domain Decomposition Methods in Science and Engineering XIX, Lect. Notes Comput. Sci. Eng 78, Springer-Verlag, New York, 2011, pp. 261–268.
[20] M. J. Gander and L. Halpern, *Absorbing boundary conditions for the wave equation and parallel computing*, Math. Comp., 74 (2004), pp. 153–176.
[21] M. J. Gander and L. Halpern, *Optimized Schwarz waveform relaxation methods for advection reaction diffusion problems*, SIAM J. Numer. Anal., 45 (2007), pp. 666–697.
[22] M. J. Gander, L. Halpern, and F. Nataf, *Optimal convergence for overlapping and non-overlapping Schwarz waveform relaxation*, in Eleventh International Conference of Domain Decomposition Methods, C.-H. Lai, P. Bjørstad, M. Cross, and O. Widlund, eds., ddm.org, 1999, pp. 27–36.
[23] M. J. Gander, L. Halpern, and F. Nataf, *Optimal Schwarz waveform relaxation for the one dimensional wave equation*, SIAM J. Numer. Anal., 41 (2003), pp. 1643–1681, https://doi.org/10.1137/S003614290139559X.
[24] M. J. Gander, S. B. Lunowa, and C. Rohde, *Consistent and asymptotic-preserving finite-volume Robin transmission conditions for singularly perturbed elliptic equations*, in Domain Decomposition Methods in Science and Engineering XXVI, Springer, Cham, 2022, pp. 443–450, https://link.springer.com/book/9783030950248.
[25] M. J. Gander, F. Magoulès, and F. Nataf, *Optimized Schwarz methods without overlap for the helmholtz equation*, SIAM J. Sci. Comput., 24 (2002), pp. 38–60, https://doi.org/10.1137/S1064827501387012.
[26] M. J. Gander and C. Rohde, *Overlapping Schwarz waveform relaxation for convection-dominated nonlinear conservation laws*, SIAM J. Sci. Comput., 27 (2005), pp. 415–439, https://doi.org/10.1137/030601090.
[27] M. J. Gander and A. M. Stuart, *Space-time continuous analysis of waveform relaxation for the heat equation*, SIAM J. Sci. Comput., 19 (1998), pp. 2014–2031, https://doi.org/10.1137/S1064827596305337.
[28] M. J. Gander and H. Zhang, *A class of iterative solvers for the Helmholtz equation: Factorizations, sweeping preconditioners, source transfer, single layer potentials, polarized traces, and optimized Schwarz methods*, SIAM Rev., 61 (2019), pp. 3–76, https://doi.org/10.1137/16M109781X.
[29] E. Giladi and H. B. Keller, *Space time domain decomposition for parabolic problems*, Numer. Math., 93 (2002), pp. 279–313.
[30] T. Goudon, S. Krell, and G. Lissoni, *DDFV method for Navier-Stokes problem with outflow boundary conditions*, Numer. Math., 142 (2019), pp. 55–102, https://doi.org/10.1007/s00211-018-1014-y.
[31] T. Goudon, S. Krell, and G. Lissoni, *Non-overlapping Schwarz algorithms for the incompressible Navier-Stokes equations with DDFV discretizations*, ESAIM Math. Model. Numer. Anal., 55 (2021), pp. 1271–1321, https://doi.org/10.1051/m2an/2021024.

[32] P. Grisvard, *Elliptic Problems in Nonsmooth Domains*, Classics in Appl. Math. 69, SIAM, Philadelphia, 1985, https://doi.org/10.1137/1.9781611972030.
[33] F. Häberlein and L. Halpern, *Optimized Schwarz waveform relaxation for nonlinear systems of parabolic type*, in Domain Decomposition Methods in Science and Engineering XXI, Lect. Notes Comput. Sci. Eng. 98, Springer, Cham, 2014, pp. 29–42.
[34] F. Haeberlein, L. Halpern, and A. Michel, *Newton-Schwarz optimised waveform relaxation Krylov accelerators for nonlinear reactive transport*, in Domain Decomposition Methods in Science and Engineering XX, Lect. Notes Comput. Sci. Eng. 91, Springer, Heidelberg, 2013, pp. 387–394.
[35] L. Halpern and J. Szeftel, *Nonlinear nonoverlapping Schwarz waveform relaxation for semilinear wave propgation*, Math. Comp., 78 (2009), pp. 865–889.
[36] R. Helmig, *Multiphase Flow and Transport Processes in the Subsurface*, Springer-Verlag, New York, 1997.
[37] A. Kurganov and G. Petrova, *Central-upwind schemes on triangular grids for hyperbolic systems of conservation laws*, Numer. Methods Partial Differential Equations, 21 (2005), pp. 536–552.
[38] O. A. Ladyženskaja, V. A. Solonnikov, and N. N. Ural'ceva, *Linear and Quasi-linear Equations of Parabolic Type*, Transl. Math. Monogr., AMS, Providence, RI, 1968.
[39] E. Lelarasmee, A. E. Ruehli, and A. L. Sangiovanni-Vincentelli, *The waveform relaxation method for time-domain analysis of large scale integrated circuits*, IEEE Trans. CAD IC Syst., 1 (1982), pp. 131–145.
[40] M. Lenzinger and B. Schweizer, *Two-phase flow equations with outflow boundary conditions in the hydrophobic-hydrophilic case*, Nonlinear Anal., 73 (2010), pp. 840–853.
[41] G. Lube, L. Mueller, and F.-C. Otto, *A non-overlapping domain decomposition method for the advection-diffusion problem*, Computing, 64 (2000), pp. 49–68.
[42] S. B. Lunowa, I. S. Pop, and B. Koren, *Linearized domain decomposition methods for two-phase porous media flow models involving dynamic capillarity and hysteresis*, Comput. Methods Appl. Mech. Engrg., 372 (2020), 113364.
[43] V. Martin, *An optimized Schwarz waveform relaxation method for the unsteady convection diffusion equation in two dimensions*, Appl. Numer. Math., 52 (2005), pp. 401–428.
[44] F. Nataf and F. Rogier, *Factorization of the convection-diffusion operator and the Schwarz algorithm*, M^3AS, 5 (1995), pp. 67–93.
[45] A. Quarteroni and A. Valli, *Domain Decomposition Methods for Partial Differential Equations*, Oxford Science Publications, Oxford, UK, 1999.
[46] H. A. Schwarz, *Über einen Grenzübergang durch alternierendes Verfahren*, Vierteljahrsschrift der Naturforschenden Gesellschaft in Zürich, 15 (1870), pp. 272–286.
[47] D. Seus, K. Mitra, I. S. Pop, F. A. Radu, and C. Rohde, *A linear domain decomposition method for partially saturated flow in porous media*, Comput. Methods. Appl. Mech. Engrg., 333 (2018), pp. 331–355.
[48] D. Seus, F. A. Radu, and C. Rohde, *A linear domain decomposition method for two-phase flow in porous media*, in Numerical Mathematics and Advanced Applications ENUMATH 2017, F. Radu, K. Kumar, I. Berre, J. Nordbotten, and I. Pop, eds., Springer-Verlag, New York, 2019, pp. 603–614.
[49] J. O. Skogestad, E. Keilegavlen, and J. M. Nordbotten, *Domain decomposition strategies for nonlinear flow problems in porous media*, J. Comput. Phys., 234 (2013), pp. 439–451.
[50] B. Smith, P. E. Bjorstad, and W. D. Gropp, *Domain Decomposition—Parallel Multilevel Methods for Elliptic Partial Differential Equations*, Cambridge University Press, Cambridge, UK, 1996.
[51] L. G. Softova and P. Weidemaier, *Quasilinear parabolic problem in spaces of maximal regularity*, J. Nonlinear Convex Anal., 7 (2006), pp. 529–540.
[52] A. Toselli and O. Widlund, *Domain Decomposition Methods—Algorithms and Theory*, Springer Ser. Comput. Math. 34, Springer, New York, 2004.
[53] E. Zeidler, *Applied Functional Analysis: Applications to Mathematical Physics*, Springer, New York, 1995.